Biomedical image reconstruction: From the foundations to deep neural nets

Michael Unser
Biomedical Imaging Group
EPFL, Lausanne, Switzerland

Pol del Aguila Pla
Center for Biomedical Imaging
Mathematical Imaging Section
EPFL, Lausanne, Switzerland

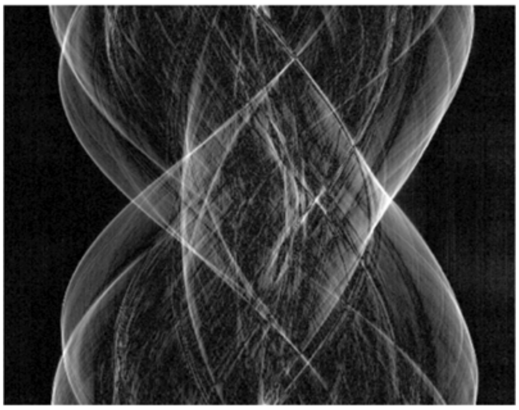

Tutorial 10, *IEEE Int. Conf. Audio, Speech & Signal Processing (ICASSP 2020),* 4-8 May 2020, Barcelona

OUTLINE

- **1. Imaging as an inverse problem**
  - Basic imaging operators
  - Discretization of the inverse problem
- **2. Classical image reconstruction** (1st gen.)
  - Backprojection
  - Tikhonov regularization; Wiener / LMSE solution
- **3. Sparsity-based image reconstruction** (2nd gen.)

GlobalBioIm

A unifying Matlab library for imaging inverse problems

Specific examples:

Magnetic resonance imaging
Computed tomography
Differential phase-contrast tomography

- **4. The learning (R)evolution** (3rd gen.)

Inverse problems in bio-imaging

- Linear forward model $\mathbf{y} = \mathbf{H}\mathbf{s} + \mathbf{n}$

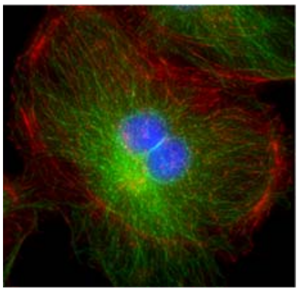

$\mathbf{s}$

noise

$\mathbf{n}$

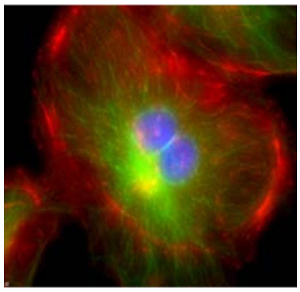

Problem: recover $\mathbf{s}$ from noisy measurements $\mathbf{y}$

- The easy scenario

  Inverse problem is **well**

  $\Rightarrow \quad \mathbf{s} \approx \mathbf{H}^{-1}\mathbf{y}$

- Backprojection (p

Basic limitations

1) Inherent noise amplification
2) Difficulty to invert **H** (too large or non-square)
3) All interesting inverse problems are **ill-posed**

Part 1:

Setting up the problem

Forward imaging model (noise-free)

Unknown molecular/anatomical map: $s(\boldsymbol{r}), \boldsymbol{r} = (x, y, z, t) \in \mathbb{R}^d$

defined over a continuum in space-time

$s \in L_2(\mathbb{R}^d)$ (space of finite-energy functions)

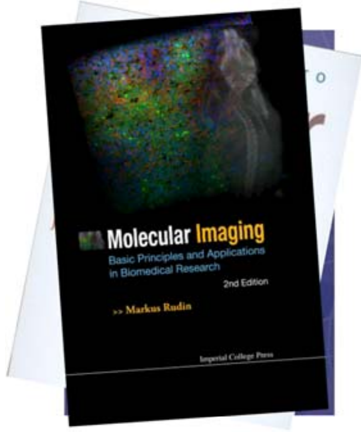

Imaging operator $\mathrm{H} : s \mapsto \mathbf{y} = (y_1, \cdots, y_M) = \mathrm{H}\{s\}$

from continuum to discrete (finite dimensional)

$\mathrm{H} : L_2(\mathbb{R}^d) \rightarrow \mathbb{R}^M$

Linearity assumption: for all $s_1, s_2 \in L_2(\mathbb{R}^d), \alpha_1, \alpha_2 \in \mathbb{R}$

$$\mathrm{H}\{\alpha_1 s_1 + \alpha_2 s_2\} = \alpha_1 \mathrm{H}\{s_1\} + \alpha_2 \mathrm{H}\{s_2\}$$

impulse response of *m*th detector

$$\Rightarrow \quad [\mathbf{y}]_m = y_m = \langle \eta_m, s \rangle = \int_{\mathbb{R}^d} \eta_m(\boldsymbol{r}) s(\boldsymbol{r}) \mathrm{d}\boldsymbol{r}$$

(by the Riesz representation theorem)

Images are obviously made of sine waves ...

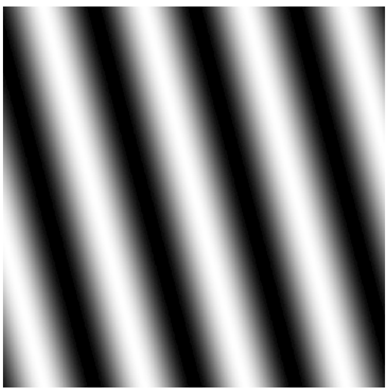

Basic operator: Fourier transform

$$\mathcal{F}: L_2(\mathbb{R}^d) \to L_2(\mathbb{R}^d)$$

$$\hat{f}(\boldsymbol{\omega}) = \mathcal{F}\{f\}(\boldsymbol{\omega}) = \int_{\mathbb{R}^d} f(\boldsymbol{x}) \mathrm{e}^{-\mathrm{j}\langle \boldsymbol{\omega}, \boldsymbol{x} \rangle} \mathrm{d}\boldsymbol{x}$$

Reconstruction formula (inverse Fourier transform)

$$f(\boldsymbol{x}) = \mathcal{F}^{-1}\{f\}(\boldsymbol{x}) = \frac{1}{(2\pi)^d} \int_{\mathbb{R}^d} \hat{f}(\boldsymbol{\omega}) e^{j\langle \boldsymbol{\omega}, \boldsymbol{r} \rangle} \mathrm{d}\boldsymbol{\omega} \qquad \text{(a.e.)}$$

Equivalent analysis functions: $\eta_m(\boldsymbol{x}) = \mathrm{e}^{\mathrm{j}\langle \boldsymbol{\omega}_m, \boldsymbol{x} \rangle}$ (complex sinusoids)

2D Fourier reconstruction

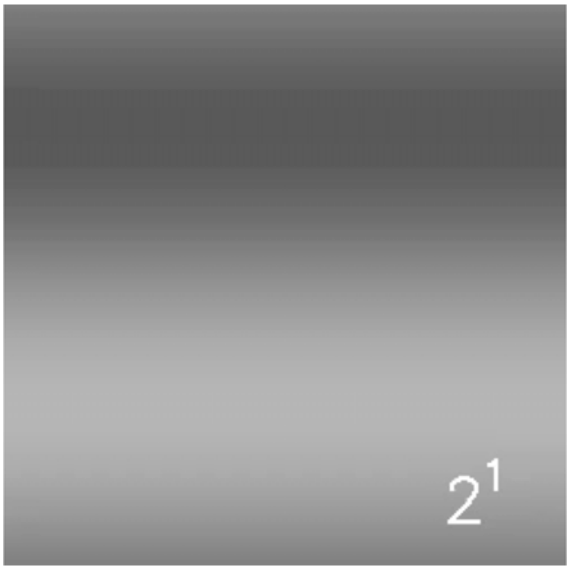

Original image:

$f(\boldsymbol{x})$

Reconstruction using N largest coefficients:

$$\tilde{f}(\boldsymbol{x}) = \frac{1}{(2\pi)^2} \sum_{\text{subset}} \hat{f}(\boldsymbol{\omega}) e^{j\langle \boldsymbol{x}, \boldsymbol{\omega} \rangle}$$

Magnetic resonance imaging

- Magnetic resonance: $\omega_0 = \gamma B_0$

  Frequency encode:

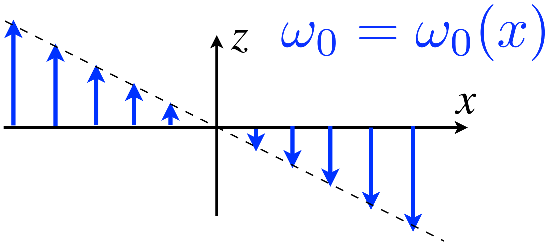

- Linear forward model for MRI

$\boldsymbol{r} = (x, y, z)$

$$\hat{s}(\boldsymbol{\omega}_m) = \int_{\mathbb{R}^3} s(\boldsymbol{r}) \mathrm{e}^{-\mathrm{j}\langle \boldsymbol{\omega}_m, \boldsymbol{r} \rangle} \mathrm{d}\boldsymbol{r}$$

(sampling of Fourier transform)

- Extended forward model with coil sensitivity

$$\hat{s}_w(\boldsymbol{\omega}_m) = \int_{\mathbb{R}^3} w(\boldsymbol{r}) s(\boldsymbol{r}) \mathrm{e}^{-\mathrm{j}\langle \boldsymbol{\omega}_m, \boldsymbol{r} \rangle} \mathrm{d}\boldsymbol{r}$$

Basic operator: Windowing

$$\mathrm{W} : L_2(\mathbb{R}^d) \to L_2(\mathbb{R}^d)$$

$$\mathrm{W}\{f\}(\boldsymbol{x}) = w(\boldsymbol{x}) f(\boldsymbol{x})$$

Positive window function (continuous and bounded): $w \in C_{\mathrm{b}}(\mathbb{R}^d), w(\boldsymbol{x}) \geq 0$

- Special case: modulation

$$w(\boldsymbol{r}) = \mathrm{e}^{\mathrm{j}\langle \boldsymbol{\omega}_0, \boldsymbol{r} \rangle}$$

$$\mathrm{e}^{\mathrm{j}\langle \boldsymbol{\omega}_0, \boldsymbol{r} \rangle} f(\boldsymbol{r}) \quad \xleftrightarrow{\mathcal{F}} \quad \hat{f}(\boldsymbol{\omega} - \boldsymbol{\omega}_0)$$

Application: Structured illumination microscopy (SIM)

Basic operator: Convolution

$$\mathrm{H} : L_2(\mathbb{R}^d) \rightarrow L_2(\mathbb{R}^d)$$

$$\mathrm{H}\{f\}(\boldsymbol{x}) = (h * f)(\boldsymbol{x}) = \int_{\mathbb{R}^d} h(\boldsymbol{x} - \boldsymbol{y}) f(\boldsymbol{y}) \mathrm{d}\boldsymbol{y}$$

Impulse response: $h(\boldsymbol{x}) = \mathrm{H}\{\delta\}$

Equivalent analysis functions: $\eta_m(\boldsymbol{x}) = h(\boldsymbol{x}_m - \cdot)$

Frequency response: $\hat{h}(\boldsymbol{\omega}) = \mathcal{F}\{h\}(\boldsymbol{\omega})$

- Convolution as a frequency-domain product

$$(h * f)(\boldsymbol{x}) \quad \xleftrightarrow{\mathcal{F}} \quad \hat{h}(\boldsymbol{\omega})\hat{f}(\boldsymbol{\omega})$$

Modeling of optical systems

$f(x, y)$

$g(x, y) = (h * f)(x, y)$

$h(x, y)$: Point Spread Function (PSF)

Diffraction-limited optics = LSI system

- Aberration-free point spread function (in focal plane)

$$h(x, y) = h(r) = C \cdot \left[\frac{2J_1(\pi r)}{\pi r}\right]^2$$

where $r = \sqrt{x^2 + y^2}$ (radial distance)

Radial profile

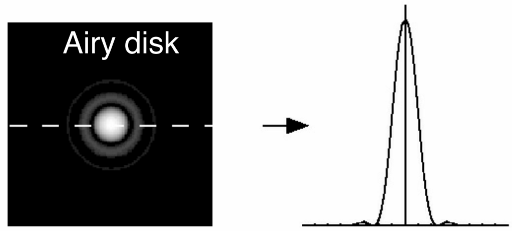

- Effect of misfocus

Point source

output

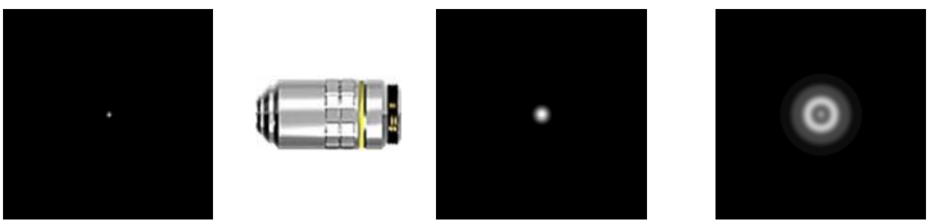

(in focus)

(defocus)

Basic operator: X-ray transform

Projection geometry: $\boldsymbol{x} = t\boldsymbol{\theta} + r\boldsymbol{\theta}^{\perp}$ with $\boldsymbol{\theta} = (\cos\theta, \sin\theta)$

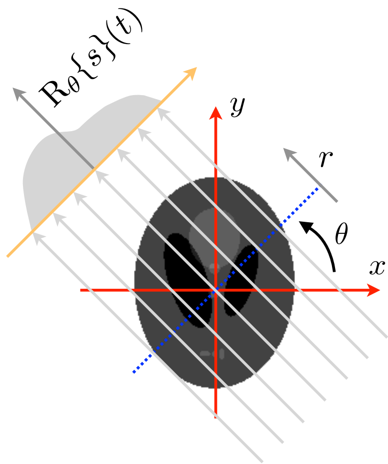

- Radon transform (line integrals)

$$\mathrm{R}_\theta\{s(\boldsymbol{x})\}(t) = \int_{\mathbb{R}} s(t\boldsymbol{\theta} + r\boldsymbol{\theta}^{\perp})\mathrm{d}r$$
$$= \int_{\mathbb{R}^2} s(\boldsymbol{x})\delta(t - \langle \boldsymbol{x}, \boldsymbol{\theta}\rangle)\mathrm{d}\boldsymbol{x}$$

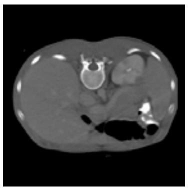

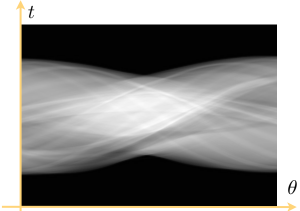

sinogram

Equivalent analysis functions: $\eta_m(\boldsymbol{x}) = \delta\big(t_m - \langle \boldsymbol{x}, \boldsymbol{\theta}_m\rangle\big)$

Central slice theorem

- Measurements of line integrals (Radon transform)

$$p_\theta(t) = \mathrm{R}_\theta\,\{f\}\,(t,\theta)$$

- 1D and 2D Fourier transforms

$$\hat{p}_\theta(\omega) = \mathcal{F}_{\mathrm{1D}}\{p_\theta\}(\omega)$$
$$\hat{f}(\boldsymbol{\omega}) = \mathcal{F}_{\mathrm{2D}}\{f\}(\boldsymbol{\omega}) = \hat{f}_{\mathrm{pol}}(\omega,\theta)$$

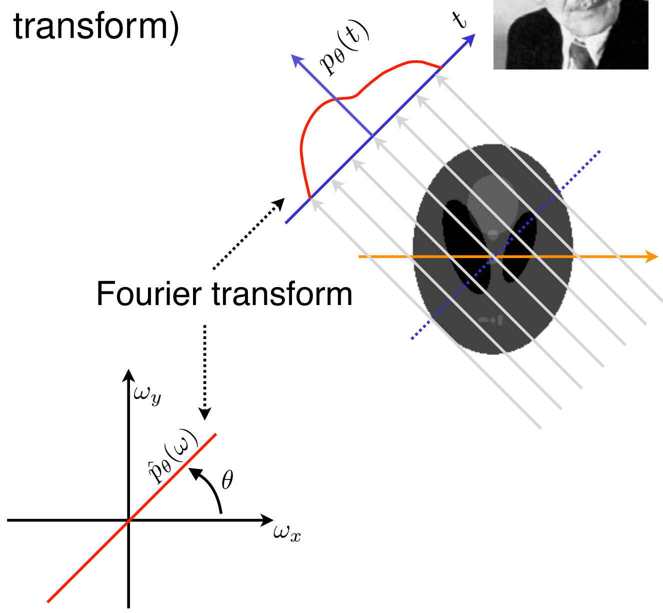

- Central-slice theorem

$$\hat{p}_\theta(\omega) = \hat{f}(\omega\cos\theta,\, \omega\sin\theta) = \hat{f}_{\mathrm{pol}}(\omega,\theta)$$

Proof: for $\theta = 0$

$$\hat{f}(\omega,0) = \int_{-\infty}^{+\infty}\int_{-\infty}^{+\infty} f(x,y)e^{-j\omega x}\,\mathrm{d}x\mathrm{d}y = \int_{-\infty}^{+\infty}\underbrace{\left(\int_{-\infty}^{+\infty} f(x,y)\,\mathrm{d}y\right)}_{p_0(x)} e^{-j\omega x}\,\mathrm{d}x = \hat{p}_0(\omega)$$

then use rotation property of Fourier transform...

Modality	Radiation	Forward model	Variations
2D or 3D tomography	coherent x-ray	$y_i = \mathrm{R}_{\boldsymbol{\theta}_i} x$	parallel, cone beam, spiral sampling
3D deconvolution microscopy	fluorescence	$y = \mathrm{H} x$	brightfield, confocal, light sheet
structured illumination microscopy (SIM)	fluorescence	$y_i = \mathrm{H}\mathrm{W}_i x$ H: PSF of microscope W_i: illumination pattern	full 3D reconstruction, non-sinusoidal patterns
Positron Emission Tomography (PET)	gamma rays	$y_i = \mathrm{H}_{\boldsymbol{\theta}_i} x$	list mode with time-of-flight
Magnetic resonance imaging (MRI)	radio frequency	$y = \mathrm{F} x$	uniform or non-uniform sampling in k space
Cardiac MRI (parallel, non-uniform)	radio frequency	$y_{t,i} = \mathrm{F}_t \mathrm{W}_i x$ W_i: coil sensitivity	gated or not, retrospective registration
Optical diffraction tomography	coherent light	$y_i = \mathrm{W}_i \mathrm{F}_i x$	with holography or grating interferometry

Discretization: Finite dimensional formalism

$$s(\boldsymbol{r}) = \sum_{\boldsymbol{k}\in\Omega} s[\boldsymbol{k}]\beta_{\boldsymbol{k}}(\boldsymbol{r})$$

Signal vector: $\mathbf{s} = \big(s[\boldsymbol{k}]\big)_{\boldsymbol{k}\in\Omega}$ of dimension K

- Measurement model (image formation)

$$y_m = \int_{\mathbb{R}^d} s(\boldsymbol{r})\eta_m(\boldsymbol{r})\mathrm{d}\boldsymbol{r} + n[m] = \langle s, \eta_m \rangle + n[m], \quad (m = 1, \dots, M)$$

η_m: sampling/imaging function (mth detector)

$n[\cdot]$: additive noise

$$\mathbf{y} = \mathbf{y}_0 + \mathbf{n} = \mathbf{H}\mathbf{s} + \mathbf{n}$$

$(M \times K)$ system matrix : $\quad [\mathbf{H}]_{m,\boldsymbol{k}} = \langle \eta_m, \beta_{\boldsymbol{k}} \rangle = \int_{\mathbb{R}^d} \eta_m(\boldsymbol{r})\beta_{\boldsymbol{k}}(\boldsymbol{r})\mathrm{d}\boldsymbol{r}$

Example of basis functions

Shift-invariant representation: $\beta_{\boldsymbol{k}}(\boldsymbol{x}) = \beta(\boldsymbol{x} - \boldsymbol{k})$

Separable generator: $\beta(\boldsymbol{x}) = \prod_{n=1}^{d} \beta(x_n)$

- Pixelated model

$$\beta(x) = \mathrm{rect}(x)$$

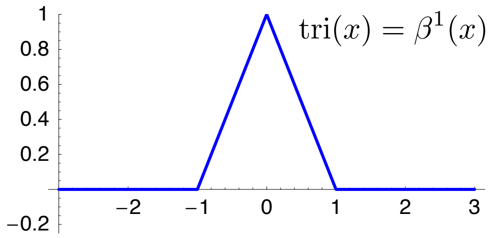

- Bilinear model

$$\beta(x) = (\mathrm{rect} * \mathrm{rect})(x) = \mathrm{tri}(x)$$

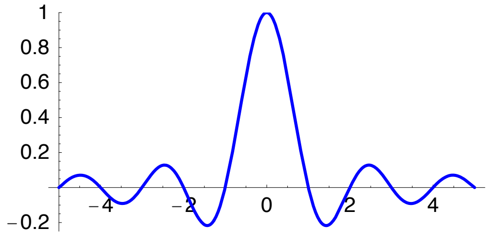

- Bandlimited representation

$$\beta(x) = \mathrm{sinc}(x)$$

Part 2:

Classical image reconstruction

Discretized forward model: **y**=**Hs**+ **n**

Inverse problem: How to efficiently recover **s** from **y** ?

Vector calculus

- Scalar cost function $J(\mathbf{v}) : \mathbb{R}^N \to \mathbb{R}$

- Vector differentiation: $\dfrac{\partial J(\mathbf{v})}{\partial \mathbf{v}} = \begin{bmatrix} \partial J / \partial v_1 \\ \vdots \\ \partial J / \partial v_N \end{bmatrix} = \nabla J(\mathbf{v})$ (gradient)

- Necessary condition for an unconstrained optimum (minimum or maximum)

$$\frac{\partial J(\mathbf{v})}{\partial \mathbf{v}} = 0$$ (also sufficient if $J(\mathbf{v})$ is convex in $\mathbf{v}$)

- Useful identities

$$\frac{\partial}{\partial \mathbf{v}}(\mathbf{a}^T\mathbf{v}) = \frac{\partial}{\partial \mathbf{v}}(\mathbf{v}^T\mathbf{a}) = \mathbf{a}$$

$$\frac{\partial}{\partial \mathbf{v}}(\mathbf{v}^T\mathbf{A}\mathbf{v}) = (\mathbf{A} + \mathbf{A}^T)\cdot\mathbf{v}$$

$$\frac{\partial}{\partial \mathbf{v}}(\mathbf{v}^T\mathbf{A}\mathbf{v}) = 2\mathbf{A}\cdot\mathbf{v}$$ if $\mathbf{A}$ is symmetric

Basic reconstruction: least-squares solution

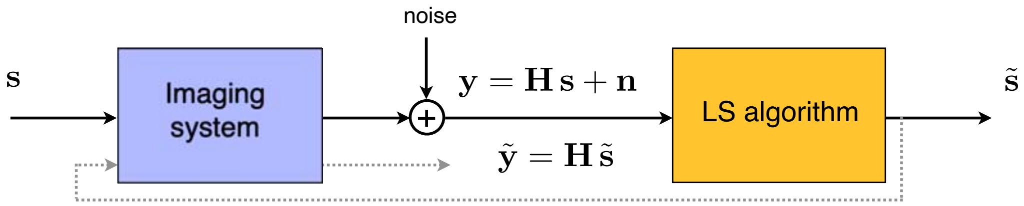

- Least-squares fitting criterion: $J_{\mathrm{LS}}(\tilde{\mathbf{s}}, \mathbf{y}) = \|\mathbf{y} - \mathbf{H}\tilde{\mathbf{s}}\|^2$

$$\min_{\tilde{\mathbf{s}}} \|\mathbf{y} - \tilde{\mathbf{y}}\|^2 = \min_{\mathbf{s}} J_{\mathrm{LS}}(\mathbf{s}, \mathbf{y})$$ (maximum consistency with the data)

- Formal least-squares solution

$$J_{\mathrm{LS}}(\mathbf{s}, \mathbf{y}) = \|\mathbf{y} - \mathbf{H}\mathbf{s}\|^2 = \|\mathbf{y}\|^2 + \mathbf{s}^T\mathbf{H}^T\mathbf{H}\,\mathbf{s} - 2\,\mathbf{y}^T\mathbf{H}\,\mathbf{s}$$

$$\frac{\partial J_{\mathrm{LS}}(\mathbf{s},\mathbf{y})}{\partial \mathbf{s}} = 2\mathbf{H}^T\mathbf{H}\mathbf{s} - 2\mathbf{H}^T\mathbf{y}$$

- Backprojection (poor m

OK if $\mathbf{H}$ is unitary $\Leftrightarrow$

Basic limitations

1) Inherent noise amplification
2) Difficulty to invert $\mathbf{H}$ (too large or non-square)
3) All interesting inverse problems are **ill-posed**

Linear inverse problems (20th century theory)

- Dealing with **ill-posed problems**: Tikhonov **regularization**

$\mathcal{R}(\mathbf{s}) = \|\mathbf{L}\mathbf{s}\|_2^2$: regularization (or smoothness) functional

$\mathbf{L}$: regularization operator (i.e., Gradient)

$$\min_{\mathbf{s}} \mathcal{R}(\mathbf{s}) \quad \text{subject to} \quad \|\mathbf{y} - \mathbf{H}\mathbf{s}\|_2^2 \le \sigma^2$$

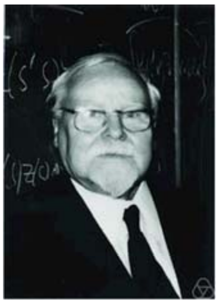

Andrey N. Tikhonov (1906-1993)

- Equivalent variational problem

$$\mathbf{s}^\star = \arg\min \underbrace{\|\mathbf{y} - \mathbf{H}\mathbf{s}\|_2^2}_{\text{data consistency}} + \underbrace{\lambda\|\mathbf{L}\mathbf{s}\|_2^2}_{\text{regularization}}$$

Formal linear solution: $\mathbf{s} = (\mathbf{H}^T\mathbf{H} + \lambda\mathbf{L}^T\mathbf{L})^{-1}\mathbf{H}^T\mathbf{y} = \mathbf{R}_\lambda \cdot \mathbf{y}$

Interpretation: "filtered" backprojection

Statistical formulation (20th century)

- Linear measurement model: $\mathbf{y} = \mathbf{H}\mathbf{s} + \mathbf{n}$

$\mathbf{n}$: additive white Gaussian noise (i. i. d.)

$\mathbf{s}$: realization of Gaussian process with zero-mean and covariance matrix $\mathbb{E}\{\mathbf{s} \cdot \mathbf{s}^T\} = \mathbf{C}_s$

Norbert Wiener (1894-1964)

- Wiener (LMMSE) solution = Gauss MMSE = Gauss MAP

$$\mathbf{s}_{\text{MAP}} = \arg\min_{\mathbf{s}} \underbrace{\frac{1}{\sigma^2}\|\mathbf{y} - \mathbf{H}\mathbf{s}\|_2^2}_{\text{Data Log likelihood}} + \underbrace{\|\mathbf{C}_s^{-1/2}\mathbf{s}\|_2^2}_{\text{Gaussian prior likelihood}}$$

$\Updownarrow \quad \mathbf{L} = \mathbf{C}_s^{-1/2}$: Whitening filter

- Quadratic regularization (Tikhonov)

$$\mathbf{s}_{\text{Tik}} = \arg\min_{\mathbf{s}} \left(\|\mathbf{y} - \mathbf{H}\mathbf{s}\|_2^2 + \lambda\mathcal{R}(\mathbf{s})\right) \quad \text{with} \quad \mathcal{R}(\mathbf{s}) = \|\mathbf{L}\mathbf{s}\|_2^2$$

Linear solution : $\mathbf{s} = (\mathbf{H}^T\mathbf{H} + \lambda\mathbf{L}^T\mathbf{L})^{-1}\mathbf{H}^T\mathbf{y} = \mathbf{R}_\lambda \cdot \mathbf{y}$

Iterative reconstruction algorithm

- Generic minimization problem: $\mathbf{s}_{\text{opt}} = \arg\min_{\mathbf{s}} J(\mathbf{s}, \mathbf{y})$
- Steepest-descent solution

$$\mathbf{s}^{(k+1)} = \mathbf{s}^{(k)} - \gamma \nabla J\big(\mathbf{s}^{(k)}, \mathbf{y}\big)$$

- Iterative constrained least-squares reconstruction

$$J_{\text{Tik}}(\mathbf{s}, \mathbf{y}) = \tfrac{1}{2}\|\mathbf{y} - \mathbf{H}\mathbf{s}\|^2 + \tfrac{\lambda}{2}\|\mathbf{L}\mathbf{s}\|^2$$

Gradient: $\dfrac{\partial J_{\text{Tik}}(\mathbf{s}, \mathbf{y})}{\partial \mathbf{s}} = -\mathbf{s}_0 + (\mathbf{H}^T\mathbf{H} + \lambda \mathbf{L}^T\mathbf{L})\mathbf{s}$ with $\mathbf{s}_0 = \mathbf{H}^T\mathbf{y}$

Steepest-descent algorithm

$$\mathbf{s}^{(k+1)} = \mathbf{s}^{(k)} + \gamma\big(\mathbf{s}_0 - (\mathbf{H}^T\mathbf{H} + \lambda \mathbf{L}^T\mathbf{L})\tilde{\mathbf{s}}^{(k)}\big)$$

Positivity constraint (IC): $[\tilde{\mathbf{s}}^{(k+1)}]_i = \begin{cases} 0, & [\mathbf{s}^{(k+1)}]_i < 0 \\ [\mathbf{s}^{(k+1)}]_i, & \text{otherwise.} \end{cases}$ (projection on convex set)

Iterative deconvolution: unregularized case

Degraded image:
Gaussian blur + additive noise

van Cittert animation

Ground truth

Effect of regularization parameter

Degraded image:
Gaussian blur + additive noise

not enough: λ=0.02

not enough: λ=0.2

Optimal regularization: λ=2

too much: λ=20

too much: λ=200

Selecting the regularization operator

- Translation, rotation and scale-invariant operators
  - Laplacian: $\Delta s = (\boldsymbol{\nabla}^T \boldsymbol{\nabla}) s \quad \longleftrightarrow \quad -\|\boldsymbol{\omega}\|^2 \hat{s}(\boldsymbol{\omega})$
  - Modulus of gradient: $|\boldsymbol{\nabla} s|$
  - Fractional Laplacian: $(-\Delta)^{\frac{\gamma}{2}} \quad \longleftrightarrow \quad \|\boldsymbol{\omega}\|^{\gamma} \hat{s}(\boldsymbol{\omega})$

- TRS-invariant regularization functional

$$\|\boldsymbol{\nabla} s\|^2_{L_2(\mathbb{R}^d)} = \|(-\Delta)^{\frac{1}{2}} s\|^2_{L_2(\mathbb{R}^d)} \qquad \Rightarrow \qquad \mathbf{L}\text{: discrete version of gradient}$$

- Fractional Brownian motion field
  - Statistical decoupling/whitening: $(-\Delta)^{\frac{\gamma}{2}} s = w \quad \longleftrightarrow \quad \frac{1}{|\boldsymbol{\omega}|^{\gamma}}$ spectral decay

Relevance of self-similarity for bio-imaging

- Fractals and physiology

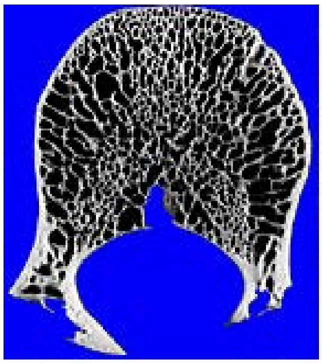

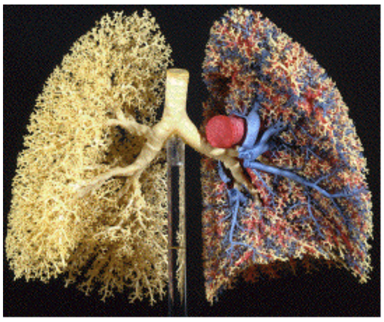

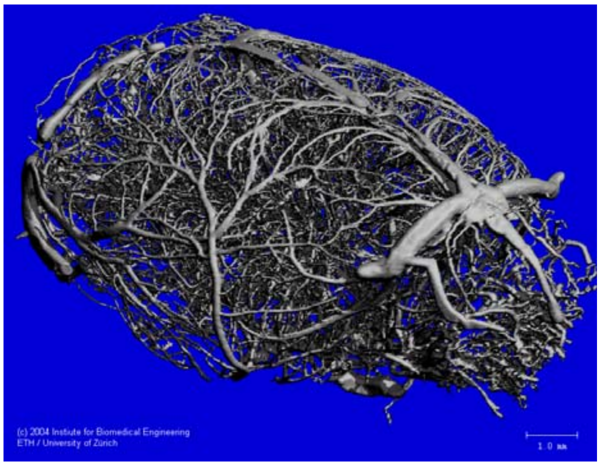

Designing fast reconstruction algorithms

Normal matrix: $\mathbf{A} = \mathbf{H}^T\mathbf{H}$ (symmetric)

Formal linear solution: $\mathbf{s} = (\mathbf{A} + \lambda \mathbf{L}^T\mathbf{L})^{-1}\mathbf{H}^T\mathbf{y} = \mathbf{R}_\lambda \cdot \mathbf{y}$

Generic form of the iterator: $\mathbf{s}^{(k+1)} = \mathbf{s}^{(k)} + \gamma\big(\mathbf{s}_0 - (\mathbf{A} + \lambda \mathbf{L}^T\mathbf{L})\mathbf{s}^{(k)}\big)$

- Recognizing structured matrices
  - $\mathbf{L}$: convolution matrix $\Rightarrow$ $\mathbf{L}^T\mathbf{L}$: symmetric convolution matrix
  - $\mathbf{L}$, $\mathbf{A}$: convolution matrices $\Rightarrow$ $(\mathbf{A} + \lambda \mathbf{L}^T\mathbf{L})$: symmetric convolution matrix

- Fast implementation
  - Diagonalization of convolution matrices $\Rightarrow$ FFT-based implementation
  - Applicable to:
    - deconvolution microscopy (Wiener filter)
    - parallel rays computer tomography (FBP)
    - MRI, including non-uniform sampling of *k*-space

Part 3:

Sparsity-based
image reconstruction
(2nd generation)

Linear inverse problems: Sparsity

(20th Century) $p = 2 \longrightarrow 1$ (21st Century)

$$\mathbf{s}_{\mathrm{rec}} = \arg\min_{\mathbf{s}} \left(\|\mathbf{y} - \mathbf{H}\mathbf{s}\|_2^2 + \lambda \mathcal{R}(\mathbf{s}) \right)$$

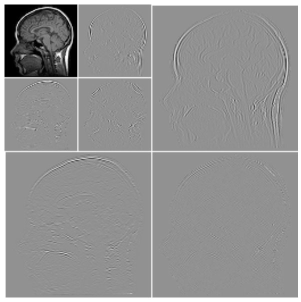

- Non-quadratic regularization regularization

$$\mathcal{R}(\mathbf{s}) = \|\mathbf{L}\mathbf{s}\|_{\ell_2}^2 \longrightarrow \|\mathbf{L}\mathbf{s}\|_{\ell_p}^p \longrightarrow \|\mathbf{L}\mathbf{s}\|_{\ell_1}$$

  - Total variation (Rudin-Osher, 1992)

    $\mathcal{R}(\mathbf{s}) = \|\mathbf{L}\mathbf{s}\|_{\ell_1}$ with $\mathbf{L}$: gradient

  - Wavelet-domain regularization (Figuereido et al., Daubechies et al. 2004)

    $\mathbf{v} = \mathbf{W}^{-1}\mathbf{s}$: wavelet expansion of $\mathbf{s}$ (typically, sparse)

    $\mathcal{R}(\mathbf{s}) = \|\mathbf{v}\|_{\ell_1}$

- Compressed sensing/sampling (Candes-Romberg-Tao; Donoho, 2006)

Sparsifying transforms

Biomedical images are well described by few basis coefficients

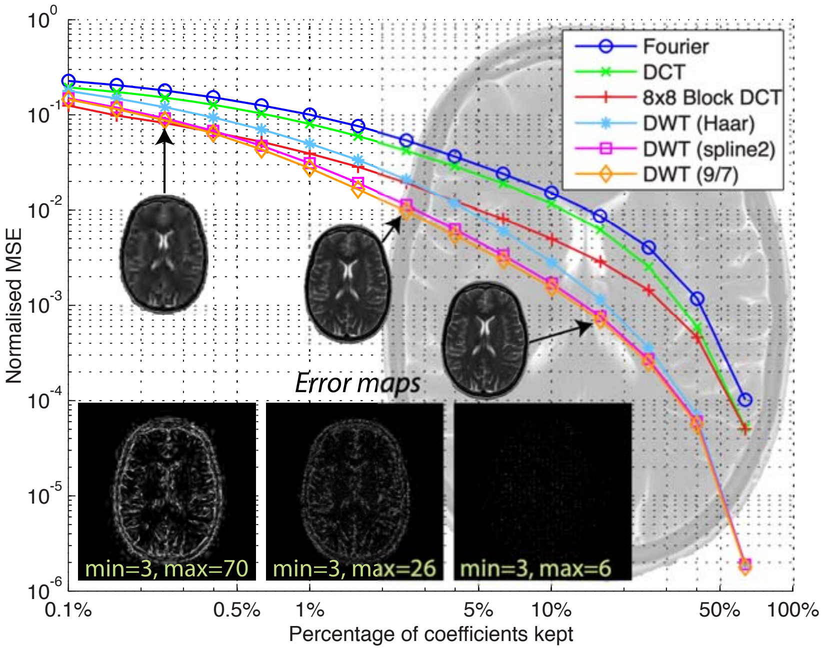

Prior = sparse representation

$$\mathcal{R}(\mathbf{s}) = \lambda \left\| \mathbf{W}^T \mathbf{s} \right\|_1$$

Advantages:
- convex
- favors sparse solutions
- Fast: WFISTA

(Guerquin-Kern *IEEE TMI* 2011)

Theory of compressive sensing

- Generalized sampling setting (after discretization)
  - Linear inverse problem: $\mathbf{y} = \mathbf{H}\mathbf{s} + \mathbf{n}$
  - Sparse representation of signal: $\mathbf{s} = \mathbf{W}\mathbf{x}$ with $\|\mathbf{x}\|_0 = K \ll N_x$
  - $N_y \times N_x$ system matrix : $\mathbf{A} = \mathbf{H}\mathbf{W}$
- Formulation of ill-posed recovery problem when $2K < N_y \ll N_x$

(P0) $\min_{\mathbf{x}} \|\mathbf{y} - \mathbf{A}\mathbf{x}\|_2^2$ subject to $\|\mathbf{x}\|_0 \le K$

- Theoretical result

Under suitable conditions on $\mathbf{A}$ (e.g., restricted isometry), the solution is unique and the recovery problem (P0) is equivalent to:

(P1) $\min_{\mathbf{x}} \|\mathbf{y} - \mathbf{A}\mathbf{x}\|_2^2$ subject to $\|\mathbf{x}\|_1 \le C_1$

[Donoho et al., 2005
Candès-Tao, 2006, ...]

Compressive sensing (CS) and l_1 minimization

[Donoho et al., 2005
Candès-Tao, 2006, ...]

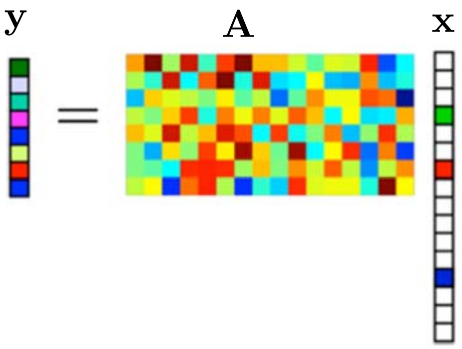

+ “noise”

Sparse representation of signal: $\mathbf{s} = \mathbf{W}\mathbf{x}$ with $\|\mathbf{x}\|_0 = K \ll N_x$

Equivalent $N_y \times N_x$ **sensing matrix** : $\mathbf{A} = \mathbf{H}\mathbf{W}$

- Constrained (synthesis) formulation of recovery problem

$$\min_{\mathbf{x}} \|\mathbf{x}\|_1 \quad \text{subject to} \quad \|\mathbf{y} - \mathbf{A}\mathbf{x}\|_2^2 \leq \sigma^2$$

Classical regularized least-squares estimator

- Linear measurement model:
  $y_m = \langle \mathbf{h}_m, \mathbf{x} \rangle + n[m], \quad m = 1, \dots, M$
- System matrix : $\mathbf{H} = [\mathbf{h}_1 \cdots \mathbf{h}_M]^T \in \mathbb{R}^{N \times N}$

$$\mathbf{x}_{\mathrm{LS}} = \arg\min_{\mathbf{x} \in \mathbb{R}^N} \|\mathbf{y} - \mathbf{H}\mathbf{x}\|_2^2 + \lambda \|\mathbf{x}\|_2^2$$

$$\Rightarrow \quad \mathbf{x}_{\mathrm{LS}} = (\mathbf{H}^T\mathbf{H} + \lambda \mathbf{I}_N)^{-1}\mathbf{H}^T\mathbf{y}$$

$$= \mathbf{H}^T\mathbf{a} = \sum_{m=1}^{M} a_m \mathbf{h}_m \quad \text{where} \quad \mathbf{a} = (\mathbf{H}\mathbf{H}^T + \lambda \mathbf{I}_M)^{-1}\mathbf{y}$$

Interpretation: $\mathbf{x}_{\mathrm{LS}} \in \mathrm{span}\{\mathbf{h}_m\}_{m=1}^M$

Lemma
$(\mathbf{H}^T\mathbf{H} + \lambda \mathbf{I}_N)^{-1}\mathbf{H}^T = \mathbf{H}^T(\mathbf{H}\mathbf{H}^T + \lambda \mathbf{I}_M)^{-1}$

Generalization: constrained l_2 minimization

- Discrete signal to reconstruct: $x = (x[n])_{n\in\mathbb{Z}}$
- Sensing operator $\mathrm{H} : \ell_2(\mathbb{Z}) \to \mathbb{R}^M$
  $x \mapsto \mathbf{z} = \mathrm{H}\{x\} = (\langle x, h_1\rangle, \dots, \langle x, h_M\rangle)$ with $h_m \in \ell_2(\mathbb{Z})$
- Closed convex set in measurement space: $\mathcal{C} \subset \mathbb{R}^M$

Example: $\mathcal{C}_{\mathbf{y}} = \{\mathbf{z} \in \mathbb{R}^M : \|\mathbf{y} - \mathbf{z}\|_2^2 \le \sigma^2\}$

Representer theorem for constrained ℓ_2 minimization

(P2) $\quad \min_{x\in\ell_2(\mathbb{Z})} \|x\|_{\ell_2}^2$ s.t. $\mathrm{H}\{x\} \in \mathcal{C}$

The problem (P2) has a unique solution of the form

$$x_{\mathrm{LS}} = \sum_{m=1}^{M} a_m h_m = \mathrm{H}^*\{\mathbf{a}\}$$

with expansion coefficients $\mathbf{a} = (a_1, \cdots, a_M) \in \mathbb{R}^M$.

(U.-Fageot-Gupta *IEEE Trans. Info. Theory*, Sept. 2016)

Constrained l_1 minimization $\Rightarrow$ sparsifying effect

- Discrete signal to reconstruct: $x = (x[n])_{n\in\mathbb{Z}}$
- Sensing operator $\mathrm{H} : \ell_1(\mathbb{Z}) \to \mathbb{R}^M$
  $x \mapsto \mathbf{z} = \mathrm{H}\{x\} = (\langle x, h_1\rangle, \dots, \langle x, h_M\rangle)$ with $h_m \in \ell_\infty(\mathbb{Z})$
- Closed convex set in measurement space: $\mathcal{C} \subset \mathbb{R}^M$

Representer theorem for constrained ℓ_1 minimization

(P1) $\quad \mathcal{V} = \arg\min_{x\in\ell_1(\mathbb{Z})} \|x\|_{\ell_1}$ s.t. $\mathrm{H}\{x\} \in \mathcal{C}$

is convex, weak*-compact with extreme points of the form

$$x_{\mathrm{sparse}}[\cdot] = \sum_{k=1}^{K} a_k \delta[\cdot - n_k] \quad \text{with} \quad K = \|x_{\mathrm{sparse}}\|_0 \le M.$$

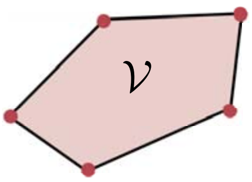

If CS condition is satisfied, then solution is unique

(U.-Fageot-Gupta *IEEE Trans. Info. Theory*, Sept. 2016)

Controlling sparsity

Measurement model: $y_m = \langle h_m, x \rangle + n[m], \quad m = 1, \ldots, M$

$$x_{\text{sparse}} = \arg \min_{x \in \ell_1(\mathbb{Z})} \left(\sum_{m=1}^{M} \left| y_m - \langle h_m, x \rangle \right|^2 + \lambda \|x\|_{\ell_1} \right)$$

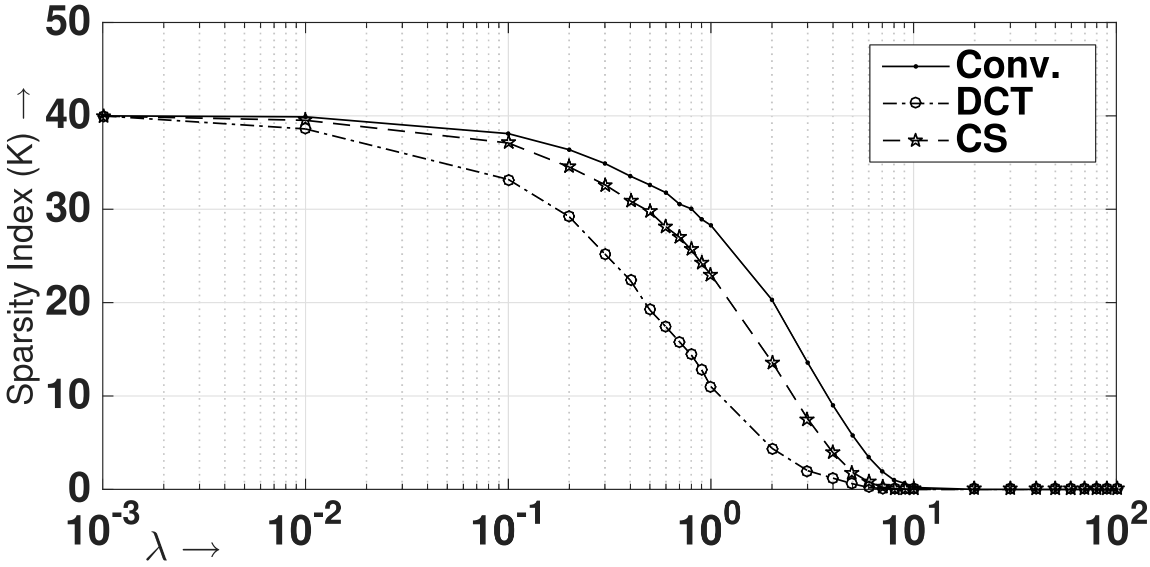

Geometry of l_2 vs. l_1 minimization

- Prototypical inverse problem

$$\min_{\mathbf{x}} \left\{ \|\mathbf{y} - \mathbf{H}\mathbf{x}\|_{\ell_2}^2 + \lambda \|\mathbf{x}\|_{\ell_2}^2 \right\} \quad \Leftrightarrow \quad \min_{\mathbf{x}} \|\mathbf{x}\|_{\ell_2} \text{ subject to } \|\mathbf{y} - \mathbf{H}\mathbf{x}\|_{\ell_2}^2 \le \sigma^2$$

$$\min_{\mathbf{x}} \left\{ \|\mathbf{y} - \mathbf{H}\mathbf{x}\|_{\ell_2}^2 + \lambda \|\mathbf{x}\|_{\ell_1} \right\} \quad \Leftrightarrow \quad \min_{\mathbf{x}} \|\mathbf{x}\|_{\ell_1} \text{ subject to } \|\mathbf{y} - \mathbf{H}\mathbf{x}\|_{\ell_2}^2 \le \sigma^2$$

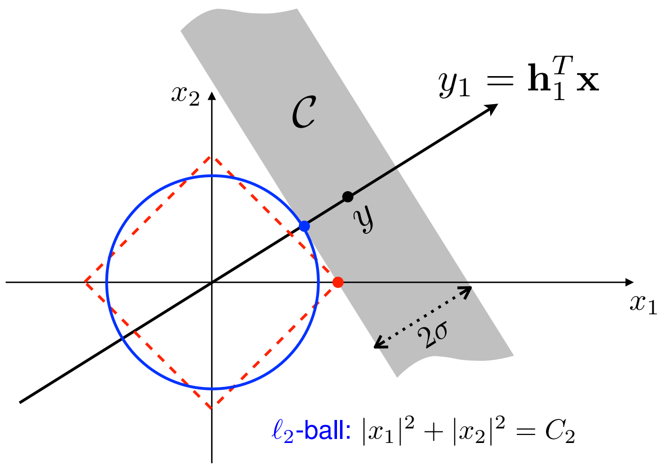

ℓ_2-ball: $|x_1|^2 + |x_2|^2 = C_2$

ℓ_1-ball: $|x_1| + |x_2| = C_1$

Geometry of l_2 vs. l_1 minimization

- Prototypical inverse problem

$$\min_{\mathbf{x}} \left\{ \|\mathbf{y}-\mathbf{H}\mathbf{x}\|_{\ell_2}^2 + \lambda \|\mathbf{x}\|_{\ell_2}^2 \right\} \Leftrightarrow \min_{\mathbf{x}} \|\mathbf{x}\|_{\ell_2} \text{ subject to } \|\mathbf{y}-\mathbf{H}\mathbf{x}\|_{\ell_2}^2 \leq \sigma^2$$

$$\min_{\mathbf{x}} \left\{ \|\mathbf{y}-\mathbf{H}\mathbf{x}\|_{\ell_2}^2 + \lambda \|\mathbf{x}\|_{\ell_1} \right\} \Leftrightarrow \min_{\mathbf{x}} \|\mathbf{x}\|_{\ell_1} \text{ subject to } \|\mathbf{y}-\mathbf{H}\mathbf{x}\|_{\ell_2}^2 \leq \sigma^2$$

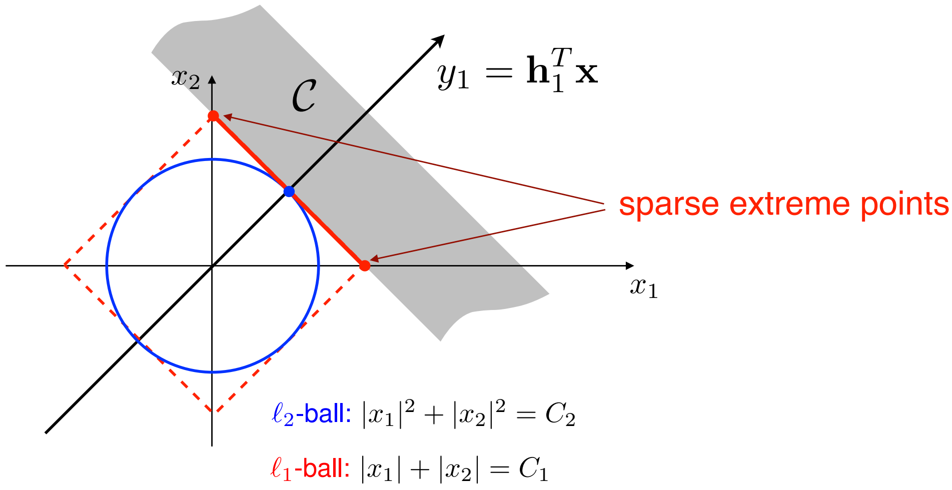

Configuration for **non-unique** ℓ_1 solution

Variational-MAP formulation of inverse problem

- Linear forward model

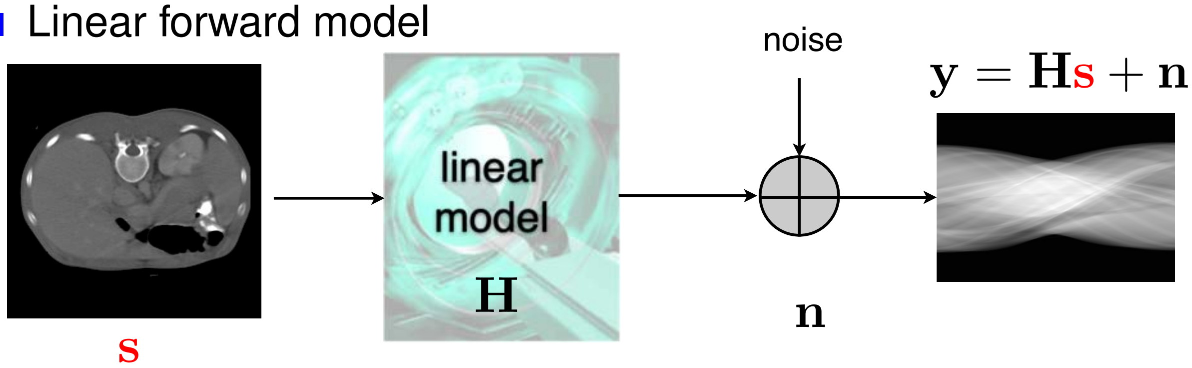

- Reconstruction as an optimization problem

$$\mathbf{s}_{\text{rec}} = \arg\min \underbrace{\|\mathbf{y}-\mathbf{H}\mathbf{s}\|_2^2}_{\text{data consistency}} + \underbrace{\lambda \|\mathbf{L}\mathbf{s}\|_p^p}_{\text{regularization}}, \quad p = 1, 2$$

$-\log \operatorname{Prob}(\mathbf{s})$: prior likelihood

Discretization of reconstruction problem

Spline-like reconstruction model: $s(\boldsymbol{r}) = \sum_{\boldsymbol{k}\in\Omega} s[\boldsymbol{k}]\beta_{\boldsymbol{k}}(\boldsymbol{r}) \quad \longleftrightarrow \quad \mathbf{s} = (s[\boldsymbol{k}])_{\boldsymbol{k}\in\Omega}$

- Statistical innovation model

$$\begin{aligned} \mathrm{L}s &= w \\ s &= \mathrm{L}^{-1}w \end{aligned}$$

Discretization

$\mathbf{u} = \mathbf{L}\mathbf{s}$ (matrix notation)

p_U is part of **infinitely divisible** family

Unser and Tafti — An Introduction to Sparse Stochastic Processes — CAMBRIDGE

- Physical model: image formation and acquisition

$$y_m = \int_{\mathbb{R}^d} s(\boldsymbol{x})\eta_m(\boldsymbol{x})\mathrm{d}\boldsymbol{x} + n[m] = \langle s, \eta_m\rangle + n[m], \quad (m = 1, \dots, M)$$

$$\mathbf{y} = \mathbf{y}_0 + \mathbf{n} = \mathbf{H}\mathbf{s} + \mathbf{n}$$

$\mathbf{n}$: i.i.d. noise with pdf p_N

Posterior probability distribution

$$\begin{aligned} p_{S|Y}(\mathbf{s}|\mathbf{y}) &= \frac{p_{Y|S}(\mathbf{y}|\mathbf{s})p_S(\mathbf{s})}{p_Y(\mathbf{y})} = \frac{p_N(\mathbf{y} - \mathbf{H}\mathbf{s})p_S(\mathbf{s})}{p_Y(\mathbf{y})} \\ &= \frac{1}{Z}p_N(\mathbf{y} - \mathbf{H}\mathbf{s})p_S(\mathbf{s}) \end{aligned}$$

(Bayes' rule)

Statistical decoupling

$$\mathbf{u} = \mathbf{L}\mathbf{s} \qquad \Rightarrow \qquad p_S(\mathbf{s}) \propto p_U(\mathbf{L}\mathbf{s}) \approx \prod_{\boldsymbol{k}\in\Omega} p_U([\mathbf{L}\mathbf{s}]_{\boldsymbol{k}})$$

- Additive white Gaussian noise scenario (AWGN)

$$p_{S|Y}(\mathbf{s}|\mathbf{y}) \propto \exp\left(-\frac{\|\mathbf{y} - \mathbf{H}\mathbf{s}\|^2}{2\sigma^2}\right) \prod_{\boldsymbol{k}\in\Omega} p_U([\mathbf{L}\mathbf{s}]_{\boldsymbol{k}})$$

... and then take the log and maximize ...

General form of MAP estimator

$$\mathbf{s}_{\mathrm{MAP}} = \operatorname{argmin} \left(\tfrac{1}{2} \|\mathbf{y} - \mathbf{H}\mathbf{s}\|_2^2 + \sigma^2 \textstyle\sum_n \Phi_U([\mathbf{L}\mathbf{s}]_n) \right)$$

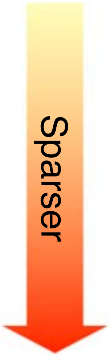

- Gaussian: $p_U(x) = \frac{1}{\sqrt{2\pi}\sigma_0} e^{-x^2/(2\sigma_0^2)}$ $\Rightarrow$ $\Phi_U(x) = \frac{1}{2\sigma_0^2} x^2 + C_1$
- Laplace: $p_U(x) = \frac{\lambda}{2} e^{-\lambda|x|}$ $\Rightarrow$ $\Phi_U(x) = \lambda|x| + C_2$
- Student: $p_U(x) = \dfrac{1}{B\left(r, \frac{1}{2}\right)} \left(\dfrac{1}{x^2+1}\right)^{r+\frac{1}{2}}$ $\Rightarrow$ $\Phi_U(x) = \left(r + \dfrac{1}{2}\right) \log(1 + x^2) + C_3$

Potential: $\Phi_U(x) = -\log p_U(x)$

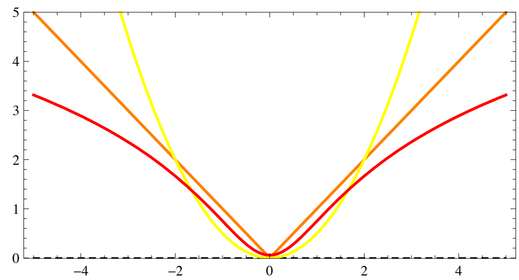

Proximal operator: pointwise denoiser

$$\operatorname{prox}_{\Phi_U}(y; \sigma^2) = \arg\min_{u \in \mathbb{R}} \frac{1}{2}|y - u|^2 + \sigma^2 \Phi_U(u)$$

$\tilde{u} = \operatorname{prox}_{\Phi_U}(y; 1)$

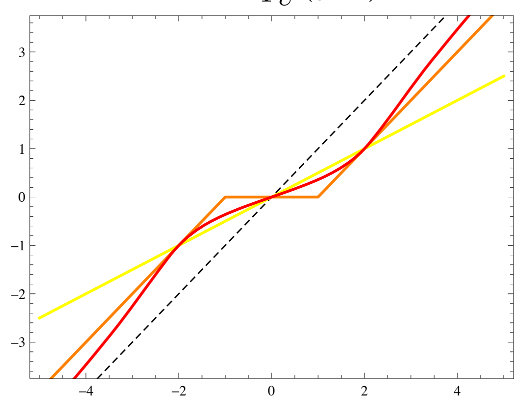

$\sigma^2 \Phi_U(u)$

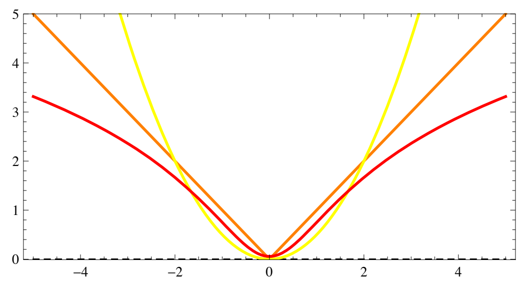

- linear attenuation — ℓ_2 minimization
- soft-threshold — ℓ_1 minimization
- shrinkage function — $\approx$ ℓ_p relaxation for $p \to 0$

Maximum a posteriori (MAP) estimation

- Constrained optimization formulation

Auxiliary **innovation** variable: $\mathbf{u} = \mathbf{L}\mathbf{s}$

$$\mathbf{s}_{\mathrm{MAP}} = \arg\min_{\mathbf{s}\in\mathbb{R}^K} \left(\frac{1}{2}\|\mathbf{y} - \mathbf{H}\mathbf{s}\|_2^2 + \sigma^2 \sum_n \Phi_U\big([\mathbf{u}]_n\big) \right) \quad \text{subject to } \mathbf{u} = \mathbf{L}\mathbf{s}$$

- Augmented Lagrangian method

Quadratic penalty term: $\frac{\mu}{2}\|\mathbf{L}\mathbf{s} - \mathbf{u}\|_2^2$

Lagrange multipler vector: $\boldsymbol{\alpha}$

$$\mathcal{L}_{\mathcal{A}}(\mathbf{s}, \mathbf{u}, \boldsymbol{\alpha}) = \frac{1}{2}\|\mathbf{y} - \mathbf{H}\mathbf{s}\|_2^2 + \sigma^2 \sum_n \Phi_U([\mathbf{u}]_n) + \boldsymbol{\alpha}^T(\mathbf{L}\mathbf{s} - \mathbf{u}) + \frac{\mu}{2}\|\mathbf{L}\mathbf{s} - \mathbf{u}\|_2^2$$

(Bostan et al. *IEEE TIP* 2013)

Alternating direction method of multipliers (ADMM)

$$\mathcal{L}_{\mathcal{A}}(\mathbf{s}, \mathbf{u}, \boldsymbol{\alpha}) = \frac{1}{2}\|\mathbf{y} - \mathbf{H}\mathbf{s}\|_2^2 + \sigma^2 \sum_n \Phi_U([\mathbf{u}]_n) + \boldsymbol{\alpha}^T(\mathbf{L}\mathbf{s} - \mathbf{u}) + \frac{\mu}{2}\|\mathbf{L}\mathbf{s} - \mathbf{u}\|_2^2$$

Sequential minimization

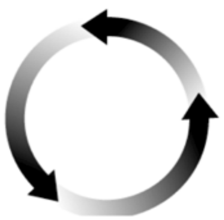

$$\mathbf{s}^{k+1} \leftarrow \arg\min_{\mathbf{s}\in\mathbb{R}^N} \mathcal{L}_{\mathcal{A}}(\mathbf{s}, \mathbf{u}^k, \boldsymbol{\alpha}^k)$$

$$\boldsymbol{\alpha}^{k+1} = \boldsymbol{\alpha}^k + \mu\big(\mathbf{L}\mathbf{s}^{k+1} - \mathbf{u}^k\big)$$

$$\mathbf{u}^{k+1} \leftarrow \arg\min_{\mathbf{u}\in\mathbb{R}^N} \mathcal{L}_{\mathcal{A}}(\mathbf{s}^{k+1}, \mathbf{u}, \boldsymbol{\alpha}^{k+1})$$

Linear inverse problem: $\mathbf{s}^{k+1} = \left(\mathbf{H}^T\mathbf{H} + \mu\mathbf{L}^T\mathbf{L}\right)^{-1}\left(\mathbf{H}^T\mathbf{y} + \mathbf{z}^{k+1}\right)$

with $\mathbf{z}^{k+1} = \mathbf{L}^T\left(\mu\mathbf{u}^k - \boldsymbol{\alpha}^k\right)$

Nonlinear denoising: $\mathbf{u}^{k+1} = \mathrm{prox}_{\Phi_U}\left(\mathbf{L}\mathbf{s}^{k+1} + \frac{1}{\mu}\boldsymbol{\alpha}^{k+1}; \frac{\sigma^2}{\mu}\right)$

- Proximal operator taylored to stochastic model

$$\mathrm{prox}_{\Phi_U}(y;\lambda) = \arg\min_u \frac{1}{2}|y-u|^2 + \lambda\Phi_U(u)$$

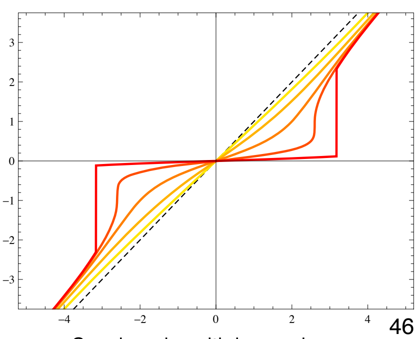

Cauchy prior with increasing s_0

Deconvolution in widefield microscopy

- Physical model of a diffraction-limited microscope

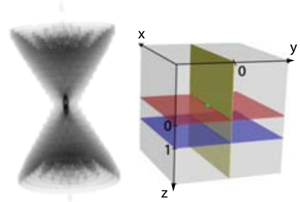

$$g(x,y,z) = (h_{3D} * s)(x,y,z)$$

3-D point spread function (PSF)

$$h_{3D}(x,y,z) = I_0 \left| p_\lambda\left(\tfrac{x}{M}, \tfrac{y}{M}, \tfrac{z}{M^2}\right)\right|^2$$

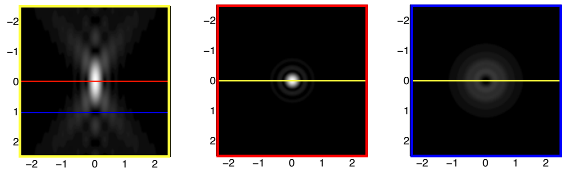

$$p_\lambda(x,y,z) = \int_{\mathbb{R}^2} P(\omega_1,\omega_2) \exp\left(\mathrm{j}2\pi z \frac{\omega_1^2+\omega_2^2}{2\lambda f_0^2}\right) \exp\left(-\mathrm{j}2\pi \frac{x\omega_1 + y\omega_2}{\lambda f_0}\right) \mathrm{d}\omega_1 \mathrm{d}\omega_2$$

Optical parameters

- λ: wavelength (emission)
- M: magnification factor
- f_0: focal length
- $P(\omega_1,\omega_2) = \mathbb{1}_{\|\boldsymbol{\omega}\|<R_0}$: pupil function
- $\mathrm{NA} = n\sin\theta = R_0/f_0$: numerical aperture

2-D (in focus) convolution model

Thin specimen $s(x,y)$ →  → $g(x,y) = (h_{2D} * s)(x,y)$

$h_{2D}(x,y)$

- Airy disk: $h_{2D}(x,y) = I_0 \left|2\frac{J_1(r/r_0)}{r/r_0}\right|^2$, with $r = \sqrt{x^2+y^2}$

$J_1(r)$: first-order Bessel function, and $r_0 = \frac{\lambda f_0}{2\pi R_0}$

Optical parameters

- λ: wavelength (emission)
- f_0: focal length
- R_0: radius of aperture

$\left|\hat{h}_{2D}(x,y)\right|$

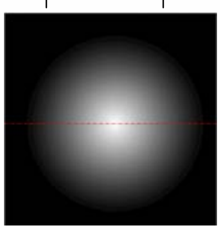

Radial profile

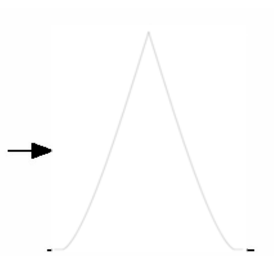

- Modulation transfer function

$$\left|\hat{h}_{2D}(\boldsymbol{\omega})\right| = \begin{cases} \frac{2}{\pi}\left(\arccos\left(\frac{\|\boldsymbol{\omega}\|}{\omega_0}\right) - \frac{\|\boldsymbol{\omega}\|}{\omega_0}\sqrt{1-\left(\frac{\|\boldsymbol{\omega}\|}{\omega_0}\right)^2}\right), & \text{for } 0 \le \|\boldsymbol{\omega}\| < \omega_0 \\ 0, & \text{otherwise} \end{cases}$$

Cut-off frequency (Rayleigh): $\omega_0 = \frac{2R_0}{\lambda f_0} = \frac{\pi}{r_0} \approx \frac{2\mathrm{NA}}{\lambda}$

2-D deconvolution: numerical set-up

- Discretization

$\boxed{\omega_0 \leq \pi}$ and representation in (separable) sinc basis

$$\beta_{\boldsymbol{k}}(\boldsymbol{x}) = \mathrm{sinc}(\boldsymbol{x} - \boldsymbol{k}) \text{ with } \boldsymbol{k} \in \mathbb{Z}^2$$

Analysis functions (impulse response): $\eta_{\boldsymbol{m}}(x, y) = h_{\mathrm{2D}}(x - m_1, y - m_2)$

$$\begin{aligned}
[\mathbf{H}]_{\boldsymbol{m},\boldsymbol{k}} &= \langle \eta_{\boldsymbol{m}}, \beta_{\boldsymbol{k}} \rangle = \langle \eta_{\boldsymbol{m}}, \mathrm{sinc}(\cdot - \boldsymbol{k}) \rangle \\
&= \langle h_{\mathrm{2D}}(\cdot - \boldsymbol{m}), \mathrm{sinc}(\cdot - \boldsymbol{k}) \rangle \\
&= \big(\mathrm{sinc} * h_{\mathrm{2D}}\big)(\boldsymbol{m} - \boldsymbol{k}) = h_{\mathrm{2D}}(\boldsymbol{m} - \boldsymbol{k}).
\end{aligned}$$

$\mathbf{H}$ and $\mathbf{L}$: convolution matrices diagonalized by discrete Fourier transform

- Linear step of ADMM algorithm implemented using the FFT

$$\mathbf{s}^{k+1} = \left(\mathbf{H}^T\mathbf{H} + \mu \mathbf{L}^T\mathbf{L}\right)^{-1} \left(\mathbf{H}^T\mathbf{y} + \mathbf{z}^{k+1}\right)$$

$$\text{with} \quad \mathbf{z}^{k+1} = \mathbf{L}^T\left(\mu \mathbf{u}^k - \boldsymbol{\alpha}^k\right)$$

2D deconvolution experiment

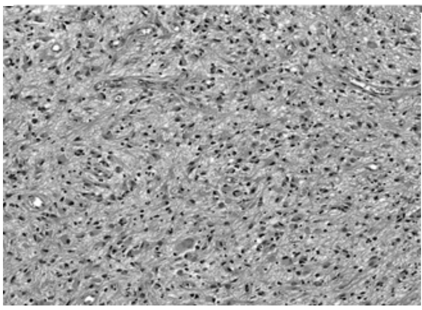

Astrocytes cells

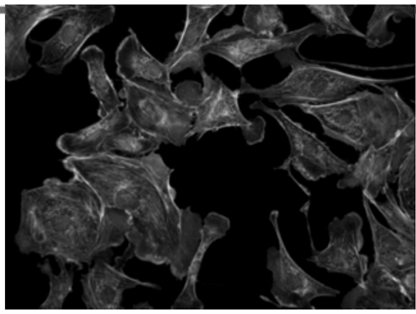

Bovine pulmonary artery cells

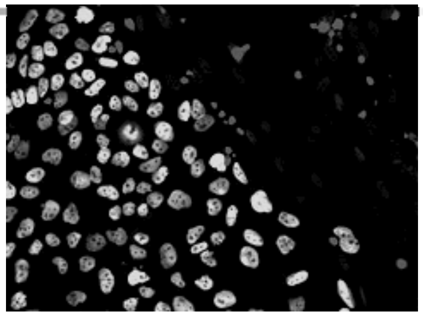

Human embryonic stem cells

Disk-shaped PSF (7×7), L: gradient (TV-like), optimized parameters

Deconvolution results (SNR in dB)

	Gaussian Estimator	Laplace Estimator	Student's Estimator
Astrocytes cells	**12.18**	10.48	10.52
Pulmonary cells	16.9	**19.04**	18.34
Stem cells	15.81	20.19	**20.5**

3D deconvolution of a widefield stack

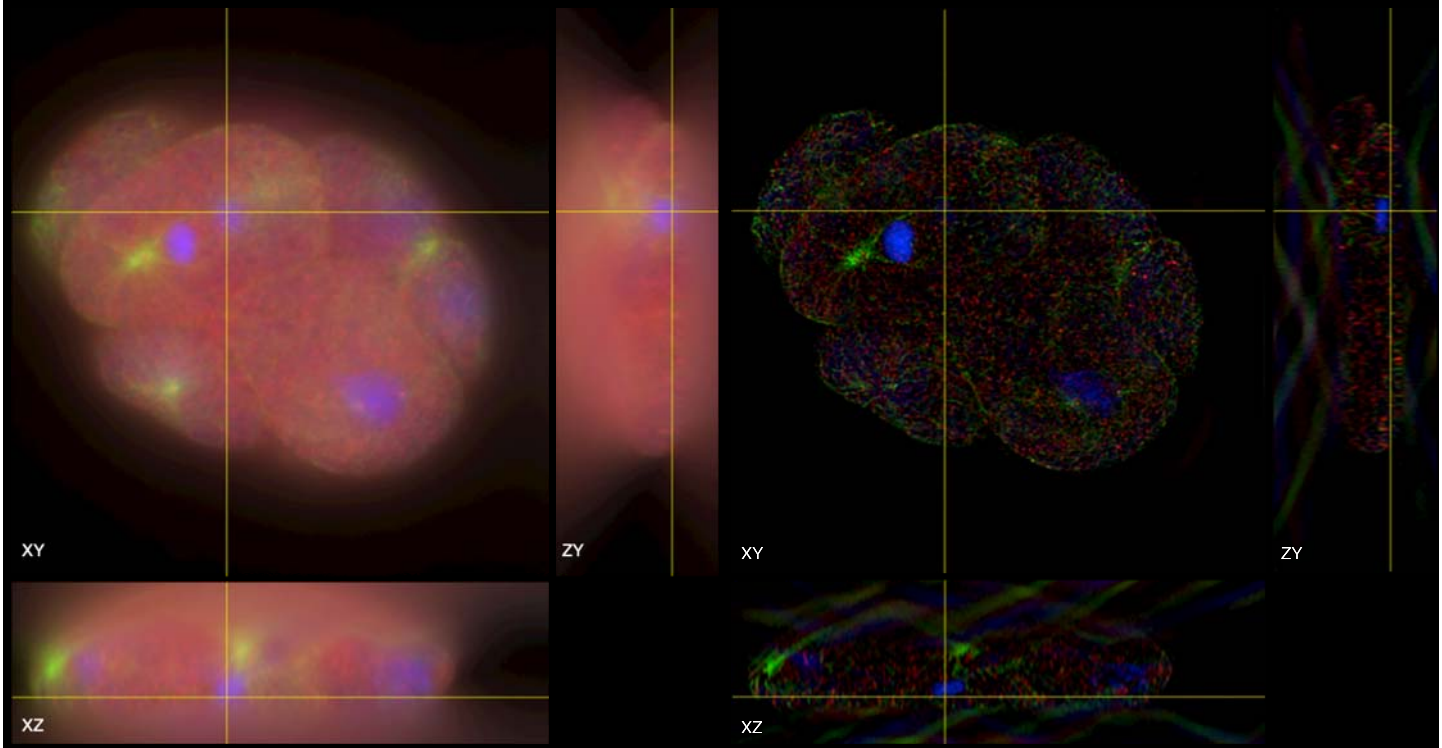

C. Elegans embryo. 3 stacks obtained by a Olympus CellR. Pixel size: 64.5 nm, Z-step: 200 nm (3.1 ratio)

PSF from an analytical model (see PSF Generator). Deconvolution with GlobalBioIm.

3D deconvolution of a widefield stack

$$\mathbf{s} = \arg\min_{\mathbf{s}\in\mathbb{R}^K} \left(\frac{1}{2} \|\mathbf{y} - \mathbf{SHs}\|_2^2 + \lambda \big\|\mathbf{Ls}\big\|_{2,1} + \delta_{\mathbb{R}_+^K}(\mathbf{s}) \right)$$

- Practical considerations
  - $\mathbf{H}$ (convolution) and $\mathbf{L}$ (gradient) as explained
  - $\mathbf{S}$: patch extraction / masking (remove padding of the FFT implementation)
  - $\|\cdot\|_{2,1}$: group-sparse norm for isotropic TV
  - $\delta_{\mathbb{R}_+^K} : \mathbb{R} \to \{0, \infty\}$: flurophore concentrations are not negative
- and more...
  - implementing proximal optimization is *hard*
  - memory management, convergence criteria, GPU?
  - efficient implementations of linear operators
  - beyond ADMM...? Trying different splittings?

erc GlobalBioIm

A unifying Matlab library for imaging inverse problems

Download/Clone the latest version

GlobalBioIm

- Three main abstract classes:
  - Linear operators (LinOp) $\underset{\text{inheritance}}{\Longrightarrow}$ LinOpConv, LinOpGrad, LinOpHess, LinOpXRay, ...
  - Cost functions (Cost) $\underset{\text{inheritance}}{\Longrightarrow}$ CostL2, CostL1, CostMixNorm12, CostNonNeg, ...
  - Optimization algorithms (Opti) $\underset{\text{inheritance}}{\Longrightarrow}$ OptiADMM, OptiChambPock, OptiGradDsct, ...

- Packaged with everything needed
  - Operators: efficient implementations of $\mathbf{Hx}$, $\mathbf{H}^*\mathbf{y}$, $\mathbf{H}^*\mathbf{Hx}$, norm, ...
  - Cost functions: gradient, prox, Lipschitz constant, ...
  - Optimization algorithms: automagically use all of the above for pain-free prototyping.

3D deconvolution of a widefield stack

$$\mathbf{s} = \arg\min_{\mathbf{s}\in\mathbb{R}^K} \left(\frac{1}{2}\|\mathbf{y} - \mathbf{SHs}\|_2^2 + \lambda \big\|\mathbf{Ls}\big\|_{2,1} + \delta_{\mathbb{R}_+^K}(\mathbf{s}) \right)$$

- ADMM with 3-way splitting
  - $\mathbf{u_1} = \mathbf{Hs}$, $\mathbf{u_2} = \mathbf{Ls}$ and $\mathbf{u_3} = \mathbf{s}$

$$\min_{\mathbf{s}\in\mathbb{R}^N} \mathcal{L}_{\mathcal{A}}\left(\mathbf{s}, \{\mathbf{u}_n^k\}_{n=1}^3, \{\boldsymbol{\alpha}_n^k\}_{n=1}^3\right) \text{ in Fourier.}$$

$$\mathcal{L}_{\mathcal{A}}\left(\mathbf{s}, \{\mathbf{u}_n\}_{n=1}^3, \{\boldsymbol{\alpha}_n\}_{n=1}^3\right) = \frac{1}{2}\|\mathbf{y} - \mathbf{Su_1}\|_2^2 + \lambda\|\mathbf{u_2}\|_{2,1} + \delta_{\mathbb{R}_+^K}(\mathbf{u_3})$$

$$+ \boldsymbol{\alpha}_1^T(\mathbf{Hs} - \mathbf{u_1}) + \frac{\mu_1}{2}\|\mathbf{Hs} - \mathbf{u_1}\|^2$$

```
% Configure convergence criteria
% 300 iterations or relative cost under 1e-4 or relative step under 1e-4
%% Run ADMM
% With initialization at zero
ADMM.run( zeros_( var_size ) );
% Configure algorithm output while running
% Report costs (1 and 2 in cost_functions, corresponding to least squares
% and TV regularizer), but don't store them, 30 times in the number of
% maximum iterations.
ADMM.OutOp    = OutputOpti( true, [], round( ADMM.maxiter / 30 ), [1, 2] );
ADMM.ItUpOut = ADMM.maxiter / 30;
least_squares_cost = l2_cost * S;
```

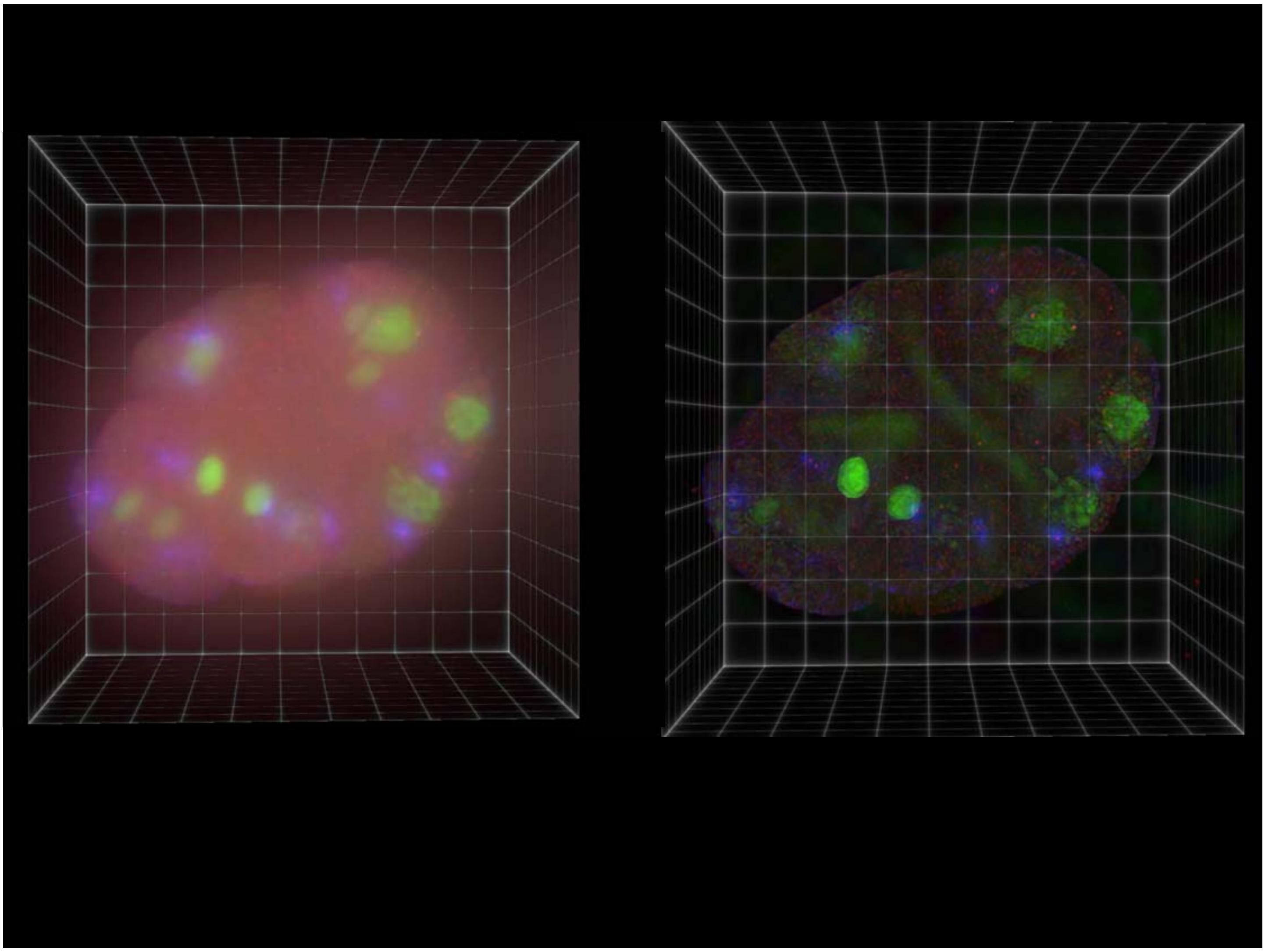

https://biomedical-imaging-group.github.io/GlobalBioIm/

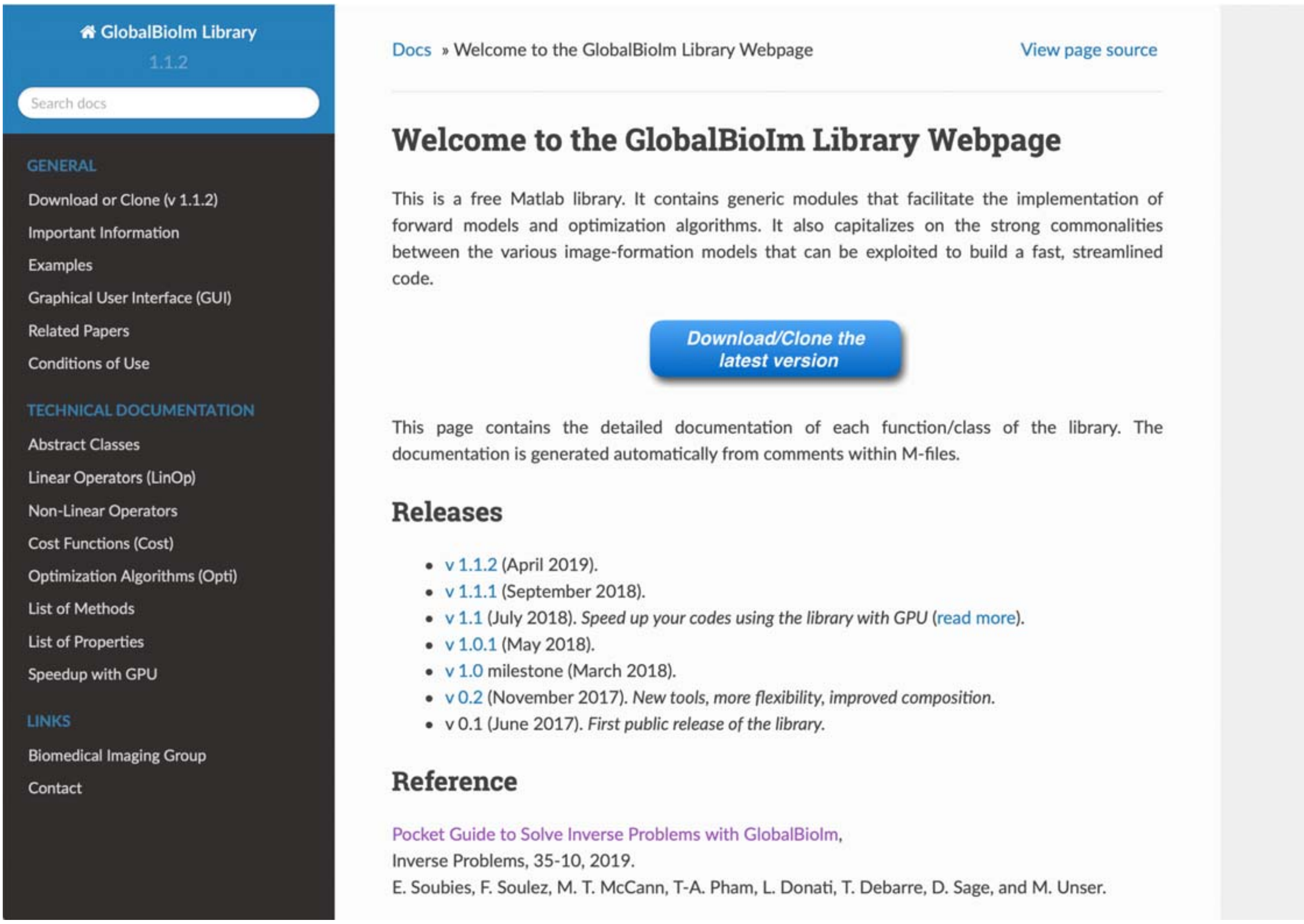

GlobalBioIm Library
1.1.2

Search docs

GENERAL
- Download or Clone (v 1.1.2)
- Important Information
- Examples
- Graphical User Interface (GUI)
- Related Papers
- Conditions of Use

TECHNICAL DOCUMENTATION
- Abstract Classes
- Linear Operators (LinOp)
- Non-Linear Operators
- Cost Functions (Cost)
- Optimization Algorithms (Opti)
- List of Methods
- List of Properties
- Speedup with GPU

LINKS
- Biomedical Imaging Group
- Contact

Docs » Welcome to the GlobalBioIm Library Webpage   View page source

Welcome to the GlobalBioIm Library Webpage

This is a free Matlab library. It contains generic modules that facilitate the implementation of forward models and optimization algorithms. It also capitalizes on the strong commonalities between the various image-formation models that can be exploited to build a fast, streamlined code.

Download/Clone the latest version

This page contains the detailed documentation of each function/class of the library. The documentation is generated automatically from comments within M-files.

Releases

- v 1.1.2 (April 2019).
- v 1.1.1 (September 2018).
- v 1.1 (July 2018). *Speed up your codes using the library with GPU* (read more).
- v 1.0.1 (May 2018).
- v 1.0 milestone (March 2018).
- v 0.2 (November 2017). *New tools, more flexibility, improved composition.*
- v 0.1 (June 2017). *First public release of the library.*

Reference

Pocket Guide to Solve Inverse Problems with GlobalBioIm,
Inverse Problems, 35-10, 2019.
E. Soubies, F. Soulez, M. T. McCann, T-A. Pham, L. Donati, T. Debarre, D. Sage, and M. Unser.

Differential phase-contrast tomography

Paul Scherrer Institute (PSI), Villigen

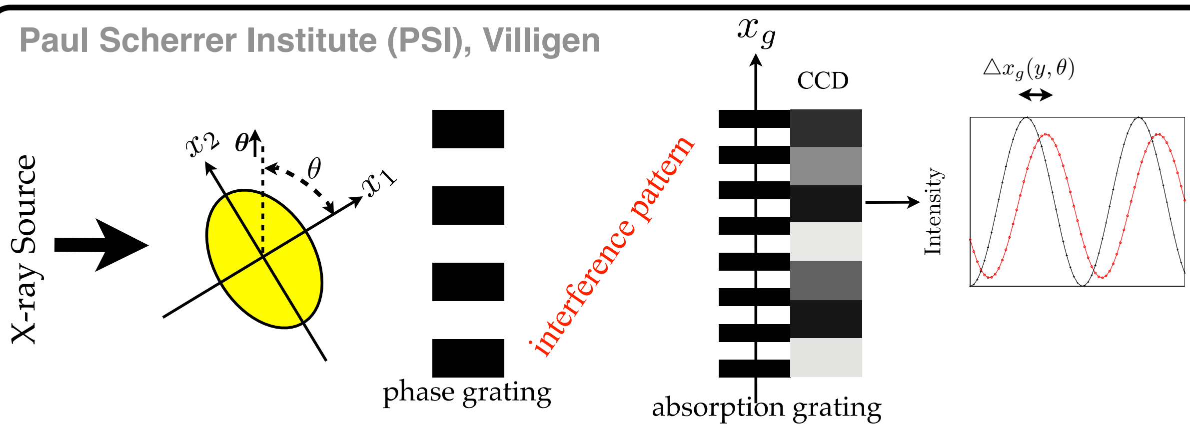

(Pfeiffer, *Nature* 2006)

Mathematical model

$$y(t,\theta) = \frac{\partial}{\partial t}\mathrm{R}_\theta\{s\}(t) \quad \longrightarrow \quad \boxed{\begin{array}{l} \mathbf{y} = \mathbf{H}\,\mathbf{s} \\ [\mathbf{H}]_{(i,j),\mathbf{k}} = \dfrac{\partial}{\partial t}\mathrm{P}_{\theta_j}\beta_{\mathbf{k}}(t_j) \end{array}}$$

Reducing the numbers of views

Rat brain reconstruction with 181 projections

ADMM-PCG

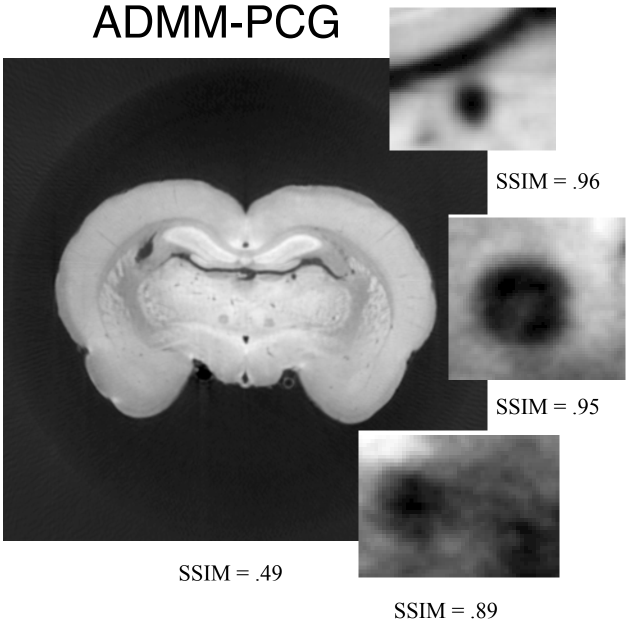

g-FBP

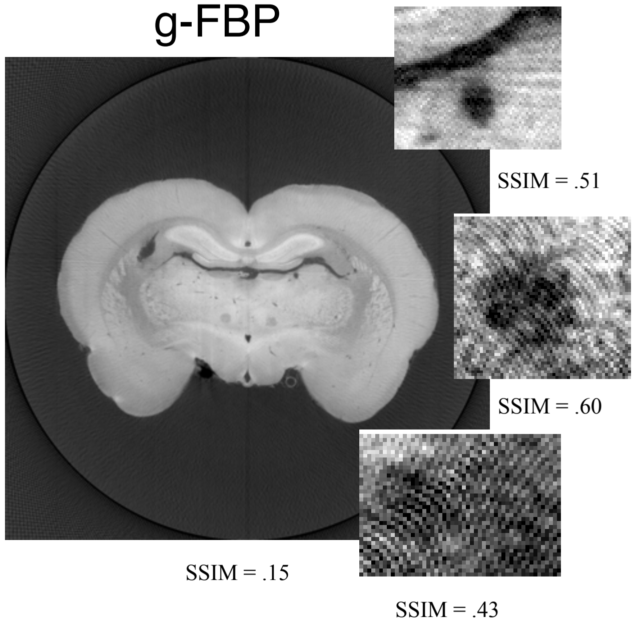

Collaboration: Prof. Marco Stampanoni, TOMCAT PSI / ETHZ

(Nichian et al. *Optics Express* 2013)

Performance evaluation

Goldstandard: high-quality iterative reconstruction with 721 views

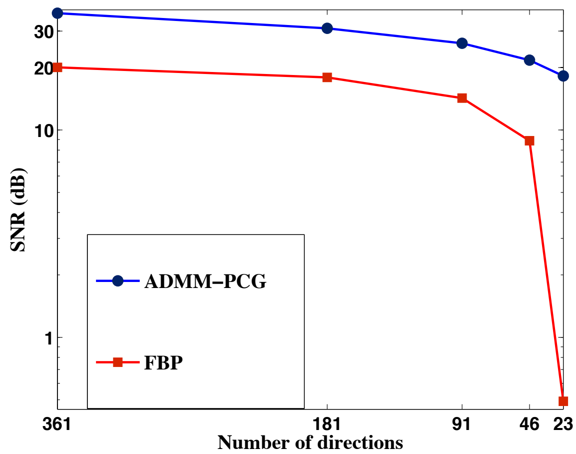

(a)

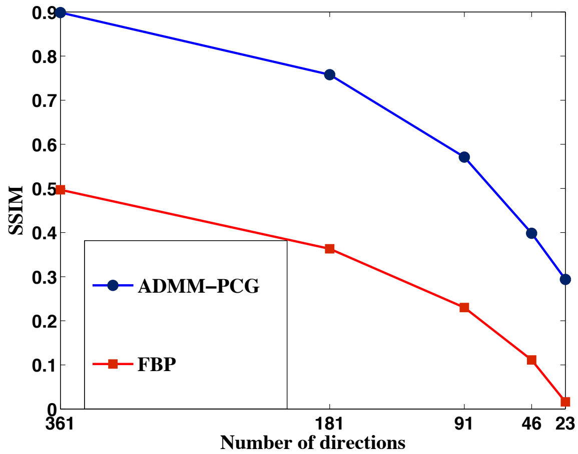

(b)

⇒ Reduction of acquisition time by a factor 10 (or more) ?

Compressed sensing: Applications in imaging

- Magnetic resonance imaging (MRI) (Lustig, *Mag. Res. Im.* 2007)

GE Healthcare PHILIPS SIEMENS

- Radio Interferometry (Wiaux, *Notic. R. Astro.* 2007)
- Teraherz Imaging (Chan, *Appl. Phys.* 2008)
- Digital holography (Brady, *Opt. Express* 2009; Marim 2010)
- Spectral-domain OCT (Liu, *Opt. Express* 2010)
- Coded-aperture spectral imaging (Arce, *IEEE Sig. Proc.* 2014)
- Localization microscopy (Zhu, *Nat. Meth.* 2012)
- Ultrafast photography (Gao, *Nature* 2014)

Conceptual summary of 2nd generation methods

$$J(\mathbf{x},\mathbf{u}) = \underbrace{\tfrac{1}{2}\|\mathbf{y}-\overset{\text{Physical model}}{\mathbf{H}}\mathbf{x}\|_2^2}_{\textit{consistency}} + \underbrace{\lambda R(\mathbf{u})}_{\textit{prior constraints}}^{\text{Statistical model of signal}} + \underbrace{\mu\|\mathbf{L}\mathbf{x}-\mathbf{u}\|_2^2}_{\textit{algorithmic coupling}}$$

Schematic structure of reconstruction algorithm:

N_{iter}

Repeat

$\mathbf{x}^{(n)} = \arg\min_{\mathbf{x}} J(\mathbf{x},\mathbf{u}^{(n-1)})$: Linear step (problem specific)

$\mathbf{u}^{(\mathbf{n})} = \arg\min_{\mathbf{u}} J(\mathbf{x}^{(n)},\mathbf{u})$: Statistical or “denoising” step

until stop criterion

Inverse problems in imaging: Current status

- **Higher reconstruction quality**: Sparsity-promoting schemes almost systematically outperform the classical linear reconstruction methods in MRI, x-ray tomography, deconvolution microscopy, etc... (Lustig et al. 2007)
- **Faster imaging, reduced radiation exposure**: Reconstruction from a lesser number of measurements supported by **compressed sensing**. (Candes-Romberg-Tao; Donoho, 2006)
- **Increased complexity**: Resolution of linear inverse problems using ℓ_1 regularization requires more sophisticated algorithms (iterative and non-linear); efficient solutions (FISTA, ADMM) have emerged during the past decade. (Chambolle 2004; Figueiredo 2004; Beck-Teboule 2009; Boyd 2011)

- Outstanding research issues
  - Beyond ℓ_1 and TV: Connection with **statistical modeling & learning**
  - Beyond matrix algebra: **Continuous-domain** formulation (Unser, *SIAM Rev* 2017)

Part 4:

The (deep) learning (r)evolution

$\Rightarrow$ Emergence of 3rd generation methods

Learning within the current paradigm

- Data-driven tuning of parameters: λ, calibration of forward model

  Semi-blind methods, sequential optimization

- Improved decoupling/representation of the signal

  Data-driven **dictionary learning** (based of sparsity or statistics/ICA) $\Rightarrow$ "optimal" $\mathbf{L}$

  (Elad 2006, Ravishankar 2011, Mairal 2012)

- Learning of non-linearities / Proximal operators

  CNN-type parametrization, backpropagation $\Rightarrow$ "optimal" potential Φ

  (Chen-Pock 2015-2016, Kamilov 2016)

Structure of iterative reconstruction algorithm

$$\mathbf{s}_{\text{sparse}} = \arg\min_{\mathbf{s}\in\mathbb{R}^K} \left(\frac{1}{2}\|\mathbf{y} - \mathbf{H}\mathbf{s}\|_2^2 + \lambda \|\mathbf{u}\|_1 \right) \text{ subject to } \mathbf{u} = \mathbf{L}\mathbf{s}$$

ADMM

$$\mathcal{L}_{\mathcal{A}}(\mathbf{s}, \mathbf{u}, \boldsymbol{\alpha}) = \frac{1}{2}\|\mathbf{y} - \mathbf{H}\mathbf{s}\|_2^2 + \lambda \sum_n |[\mathbf{u}]_n| + \boldsymbol{\alpha}^T(\mathbf{L}\mathbf{s} - \mathbf{u}) + \frac{\mu}{2}\|\mathbf{L}\mathbf{s} - \mathbf{u}\|_2^2$$

For $k = 0, \ldots, K$

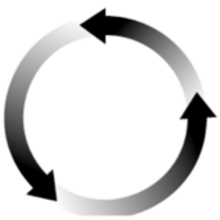

Linear step

$$\mathbf{s}^{k+1} = \left(\mathbf{H}^T\mathbf{H} + \mu\mathbf{L}^T\mathbf{L}\right)^{-1}\left(\mathbf{z}_0 + \mathbf{z}^{k+1}\right)$$

with $\mathbf{z}^{k+1} = \mathbf{L}^T\left(\mu\mathbf{u}^k - \boldsymbol{\alpha}^k\right)$

$$\boldsymbol{\alpha}^{k+1} = \boldsymbol{\alpha}^k + \mu\left(\mathbf{L}\mathbf{s}^{k+1} - \mathbf{u}^k\right)$$

Nonlinear step $\approx$ "denoising" of $\mathbf{u}$

$$\mathbf{u}^{k+1} = \text{prox}_{|\cdot|}\left(\mathbf{L}\mathbf{s}^{k+1} + \tfrac{1}{\mu}\boldsymbol{\alpha}^{k+1}; \tfrac{\lambda}{\mu}\right)$$

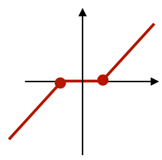

Connection with deep neural networks

(Gregor-LeCun 2010)

Unrolled Iterative Shrinkage Thresholding Algorithm (ISTA)

LISTA : learning-based ISTA

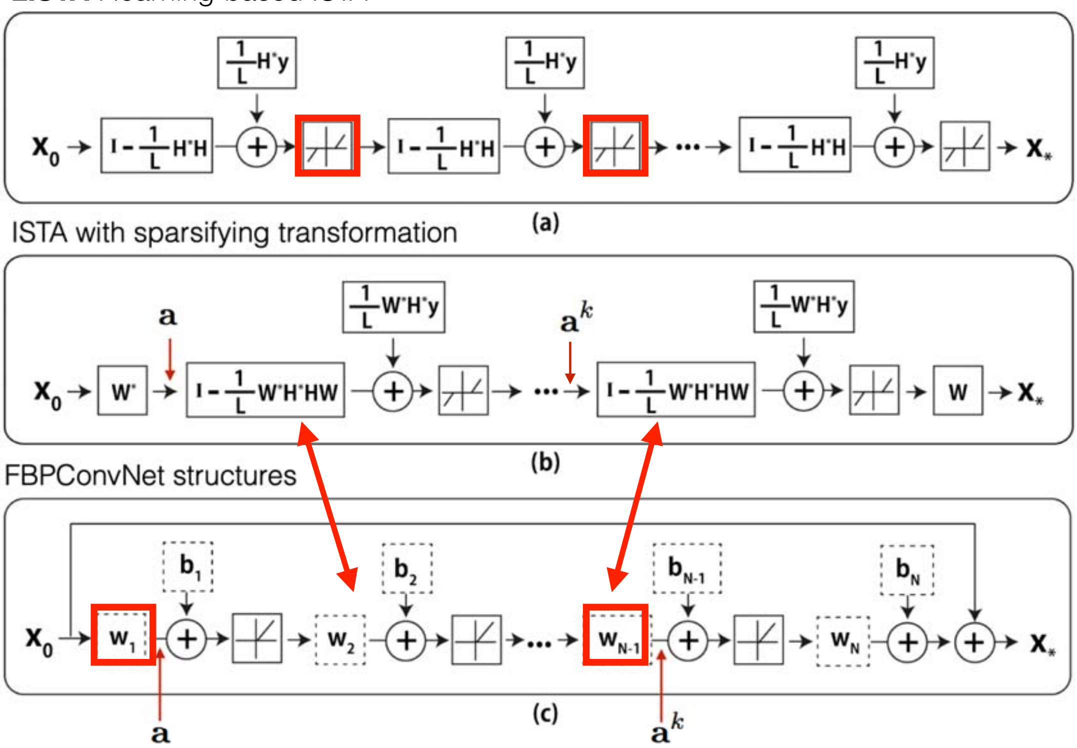

Recent appearance of Deep ConvNets

(Jin et al. 2016; Adler-Öktem 2017; Chen et al. 2017; ...)

- CT reconstruction based on Deep ConvNets
  - Input: Sparse view FBP reconstruction
  - Training: Set of 500 high-quality full-view CT reconstructions
  - Architecture: U-Net with skip connection

(Jin et al., IEEE TIP 2017)

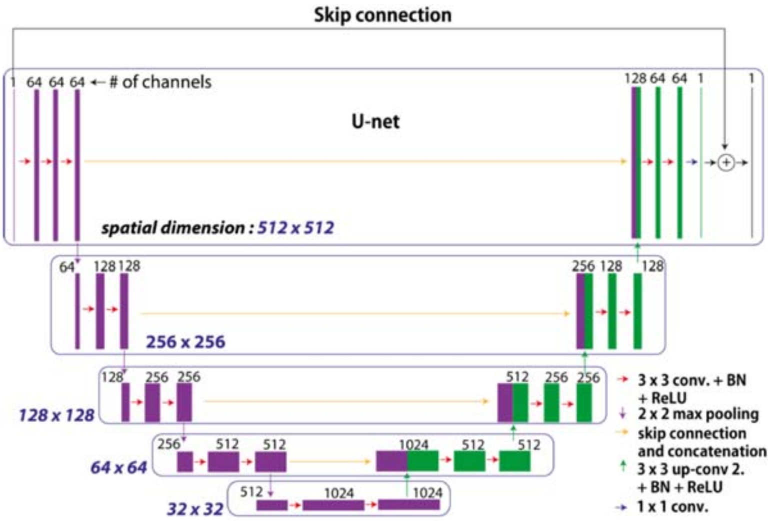

CT data

Dose reduction by 7: 143 views

Ground truth | FBP SNR 24.06 | TV SNR 29.64

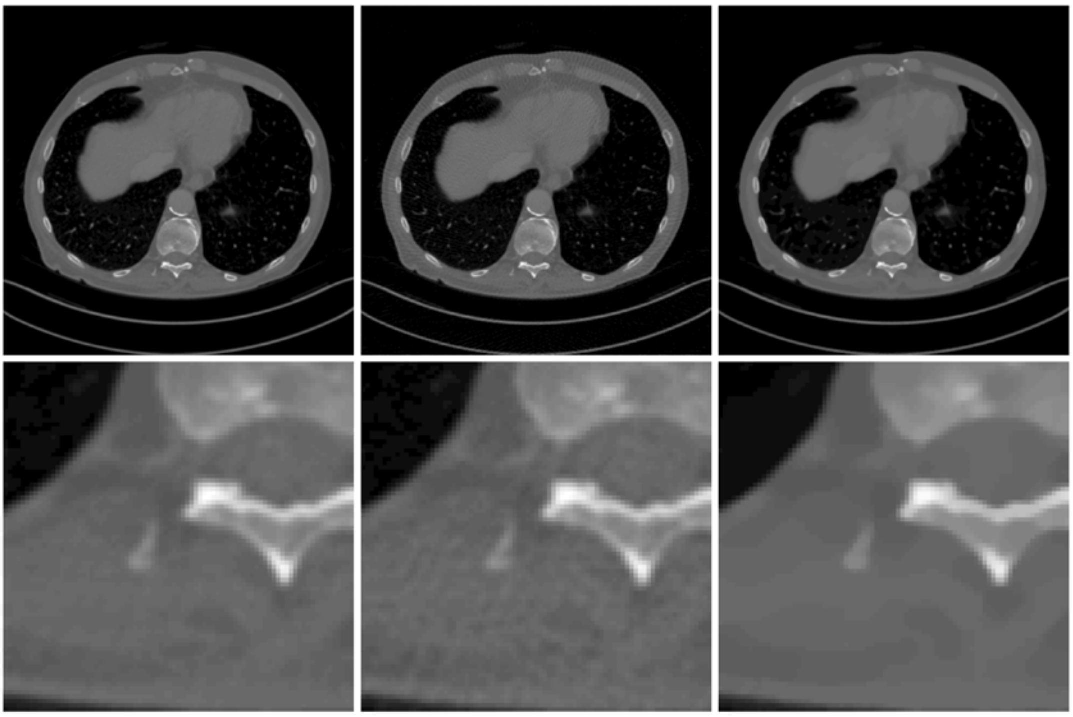

Reconstructed from
from 1000 views

MAYO CLINIC

CT data

Dose reduction by 7: 143 views

Ground truth	FBP SNR 24.06	TV SNR 29.64	FBPConvNet SNR 35.38

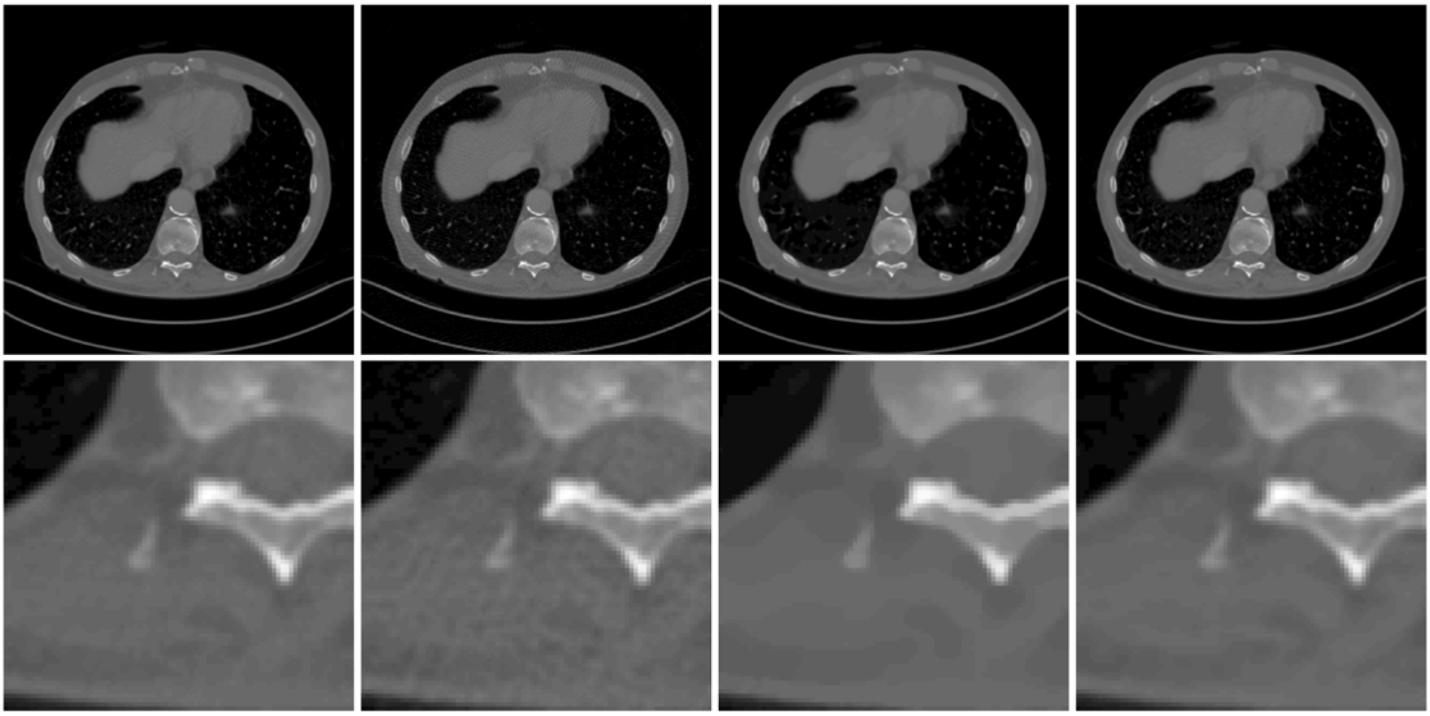

Reconstructed from from 1000 views

MAYO CLINIC

(Jin et al., *IEEE Trans. Im Proc.*, 2017)

2019 Best Paper Award
IEEE Signal Processing Society

CT data

Dose reduction by 20: 50 views

Ground truth	FBP SNR 13.43	TV SNR 24.89	FBPConvNet SNR 28.53

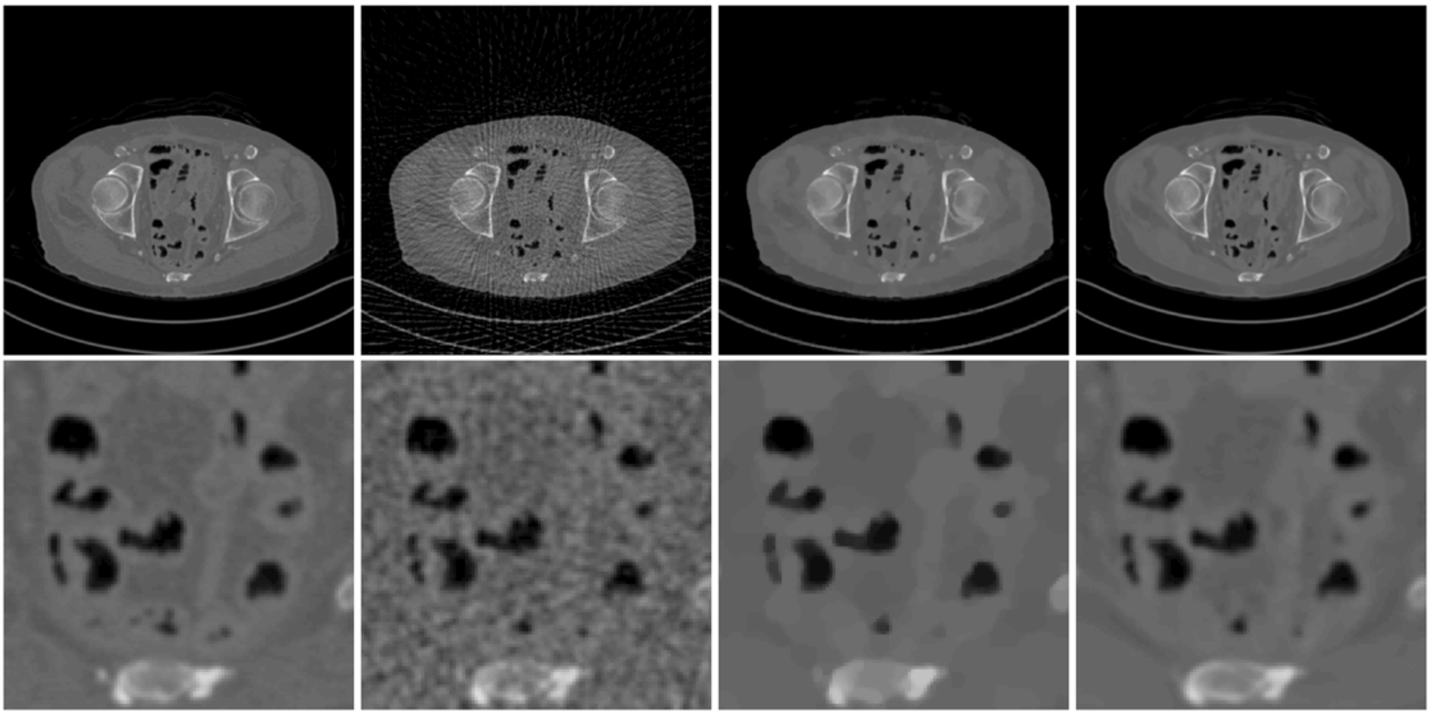

Reconstructed from from 1000 views

MAYO CLINIC

(Jin-McCann-Froustey-Unser, *IEEE Trans. Im Proc.*, 2017) *μ*CT data

Dose reduction by 14: 51 views

Ground truth	FBP SNR 3.265	TV SNR 7.481	FBPConvNet SNR 9.003

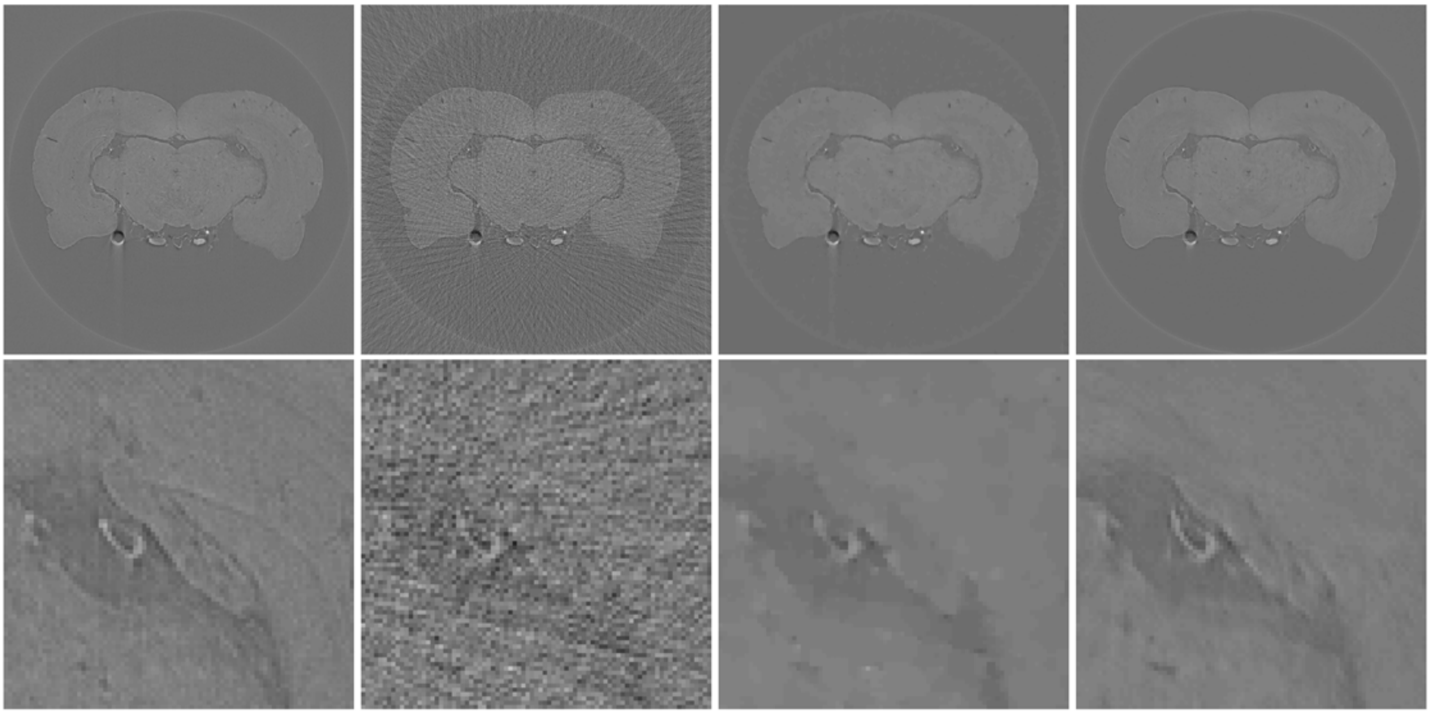

Reconstructed from
from 721 views

PAUL SCHERRER INSTITUT

COMPARISON OF SNR BETWEEN DIFFERENT RECONSTRUCTION ALGORITHMS FOR EXPERIMENTAL DATASET.

Metrics \ Methods		FBP	TV [13]	Proposed
avg. SNR (dB)	145 views (x5)	5.38	8.25	11.34
	51 views (x14)	3.29	7.25	8.85

CNN algorithms: Conditions of utilization

- Standard “regression” setting
  - Mapping of an image into an image $\boldsymbol{f_\theta} : \mathbb{R}^N \to \mathbb{R}^N : \mathbf{y} \mapsto \mathbf{s} = \boldsymbol{f_\theta}(\mathbf{y})$

- Fundamental change of paradigm

  Requires **extensive sets of representative training data**
  together with **gold-standards** = desired high-quality reconstruction

- Application niches
  - Denoising
  - Super-resolution (data extrapolation)
  - Reconstruction from **fewer measurements**
    (trained on high-quality full-view data sets)
  - Use of CNN to **emulate/speedup** some well-performing, but “slow”, reference reconstruction methods

Design of CNN algorithms: General principles

- Data preparation
  - Backprojection or classical linear reconstruction
    - $\Rightarrow$ Use of feedforward CNN to **correct artifacts** of first-generation methods

- Connection with second-generation methods
  - Conceptual: **unrolling** to justify deep architecture
  - **Hybrid** methods ("plug & play"):
    Enforce consistency, while using CNN as "regularizer" or projector
    (Tezcan···Konukoglu, *IEEE TMI* 2018)
    (Gupta···Unser, *IEEE TMI* 2018)

- Training
  - Choice of suitable cost: SNR or perceptual loss
  - Availability of extensive data set: $(\mathbf{s}_k, \mathbf{y}_k), k = 1, \dots, K$
  - Use of data augmentation: translations, rotations, deformations

Deep CNNs for bioimage reconstruction images

- X-ray tomography — (Jin···Unser, *IEEE TIP* 2017) (Chen···Wang, *Biomed Opt. Exp* 2017)
- Magnetic resonance imaging (MRI) — (Hammernik···Pock, *Mag Res Med* 2018) (Tezcan···Konukoglu, *IEEE TMI* 2018)
- Dynamic MRI (cardial imaging) — (Schlemper···Rueckert, *IEEE TMI 2018*) (Hauptmann···Arridge, *Mag Res Med* 2019)
- 2D microscopy — (Rivenson···Ozcan, *Optica* 2017)
- 3D fluorescence microscocopy — (Weigert···Jug, Myers, *Nature Meth. 2018*)
- Super-resolution microscopy — (Nehme···Shechtman, *Optica* 2018)
- Diffraction tomography — (Sun···Kamilov, *Optics Express* 2018)
- Ultrasound — (Yoon···Ye, *IEEE TMI* 2019)

Example: MRI reconstruction

Group of Thomas Pock, Univ. Graz

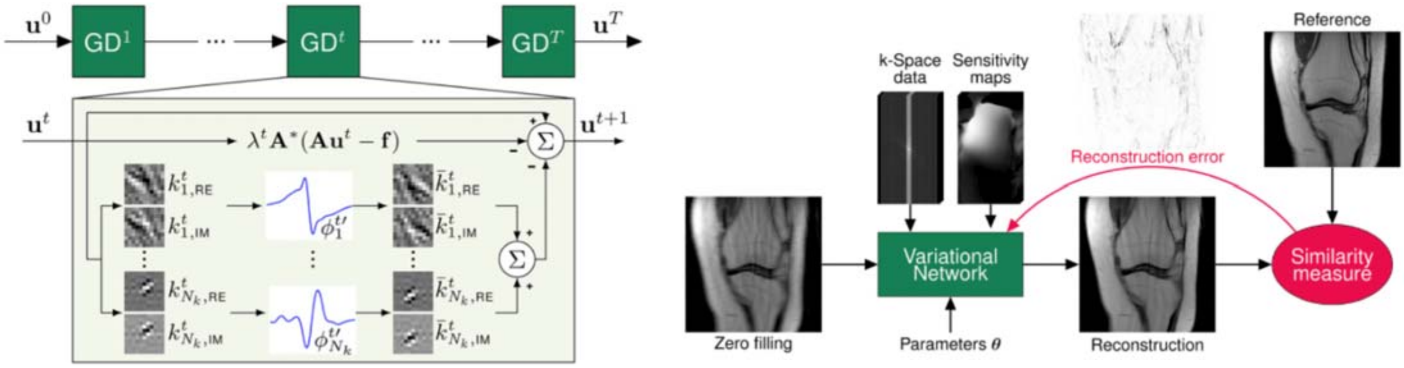

Hammernik, Kerstin, et al. "Learning a variational network for reconstruction of accelerated MRI data", *Magnetic Resonance in Medicine* 79.6 (2018): 3055-3071.

Example: Dynamic MRI reconstruction

Group of Simon Arridge, UCL

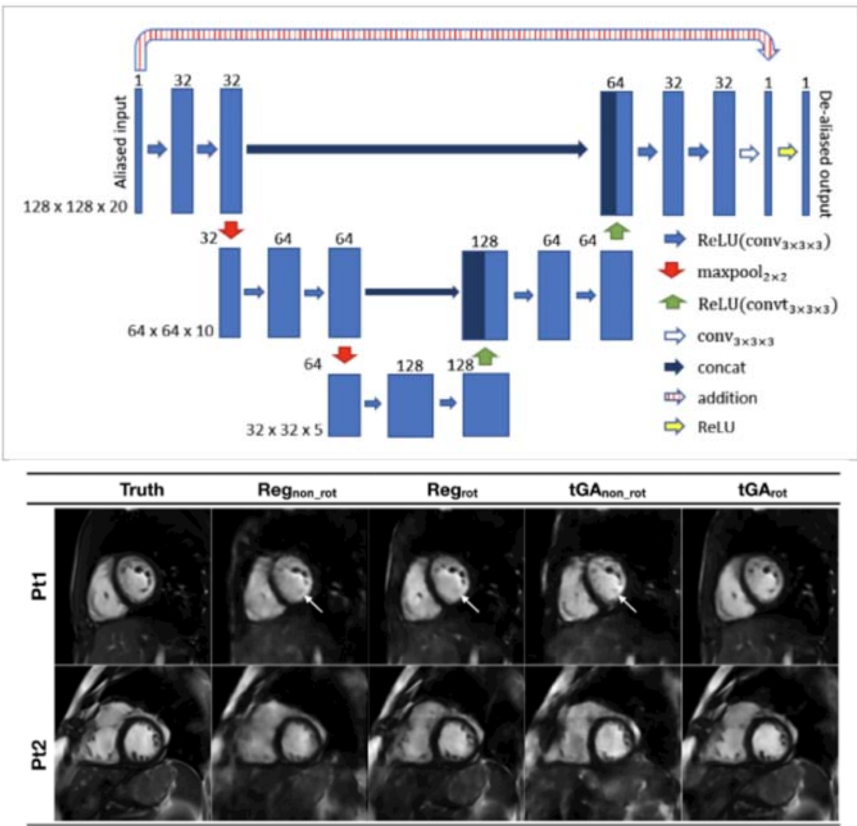

(Hauptmann et al., *Mag Res Med* 2019)

Example: Axial super-resolution in 3D fluorescence microscopy

Group of Florian Jug, Max Planck, Desden

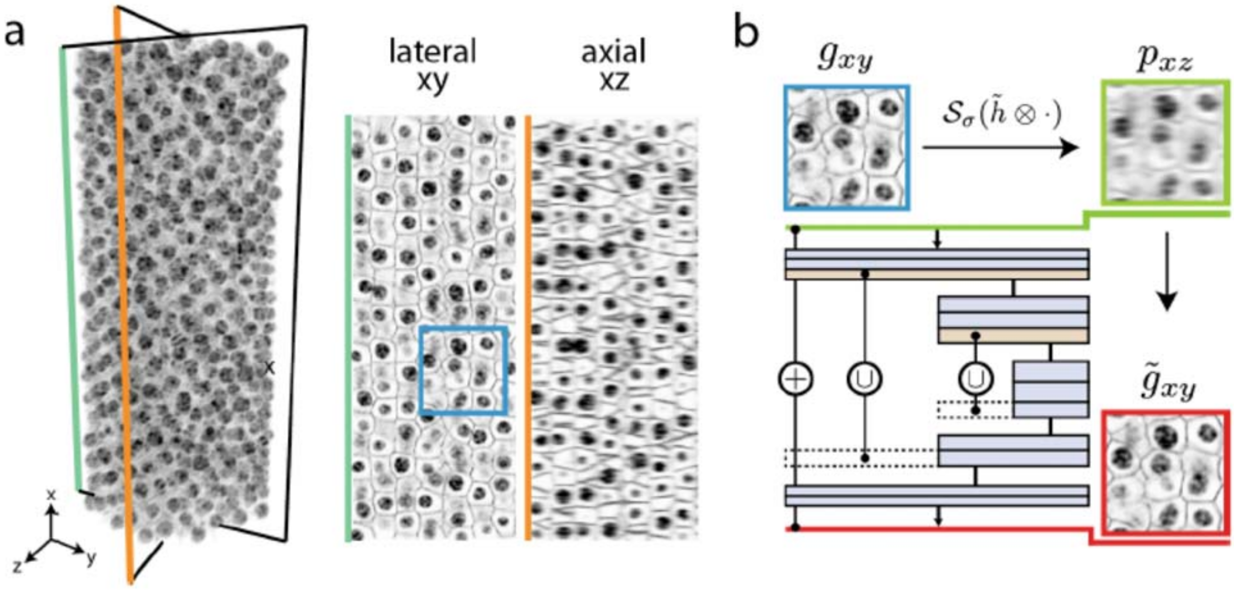

Weigert et al. "Isotropic reconstruction of 3D fluorescence microscopy images using convolutional neural networks", MICCAI, 2017.

Learning the **complete** sensor-to-image map, including the **physics** !

LETTER

Nature, March 2018

doi:10.1038/nature25988

Image reconstruction by domain-transform manifold learning

Bo Zhu[1,2,3], Jeremiah Z. Liu[4], Stephen F. Cauley[1,2], Bruce R. Rosen[1,2] & Matthew S. Rosen[1,2,3]

Image reconstruction is essential for imaging applications across the physical and life sciences, including optical and radar systems, magnetic resonance imaging, X-ray computed tomography, positron emission tomography, ultrasound imaging and radio astronomy[1–3]. During image acquisition, the sensor encodes an intermediate representation of an object in the sensor domain, which is subsequently reconstructed into an image by an inversion of the encoding function. Image reconstruction is challenging because analytic knowledge of the exact inverse transform may not exist *a priori*, especially in the presence of sensor non-idealities and noise. Thus, the standard reconstruction approach involves approximating the inverse function with multiple *ad hoc* stages in a signal processing chain[4,5], the composition of which depends on the details of each acquisition strategy, and often requires expert parameter tuning to optimize reconstruction performance. Here we present a unified framework for image reconstruction—automated transform by manifold approximation (AUTOMAP)—which recasts image reconstruction as a data-driven supervised learning task that allows a mapping between the sensor and the image domain to emerge from an appropriate corpus of training data. We implement AUTOMAP with a deep neural network and exhibit its flexibility in learning reconstruction transforms for various magnetic resonance imaging acquisition strategies, using the same network architecture and hyperparameters. We further demonstrate that manifold learning during training results in sparse representations of domain transforms along low-dimensional data manifolds, and observe superior immunity to noise and a reduction in reconstruction artefacts compared with conventional handcrafted reconstruction methods. In addition to improving the reconstruction performance of existing acquisition methodologies, we anticipate that AUTOMAP and other learned reconstruction approaches will accelerate the development of new acquisition strategies across imaging modalities.

Inspired by the perceptual learning archetype, we describe here a data-driven unified image reconstruction approach, which we call AUTOMAP, that learns a reconstruction mapping between the sensor-domain data and image-domain output (Fig. 1a). As this mapping is trained, a low-dimensional joint manifold of the data in both domains is implicitly learned (Fig. 1b), capturing a highly expressive representation that is robust to noise and other input perturbations.

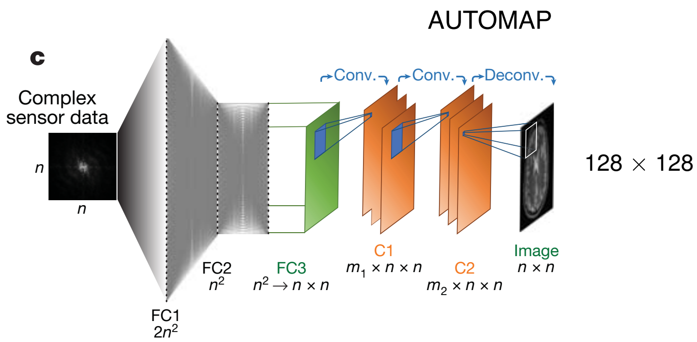

Fundamental limitation: $O(n^{2d})$ memory requirement $\Rightarrow$ Does not scale well !

DANGER

Deep networks can behave erratically (**instability**)

Tiny adversarial perturbations of increasing strength

Ground-Truth

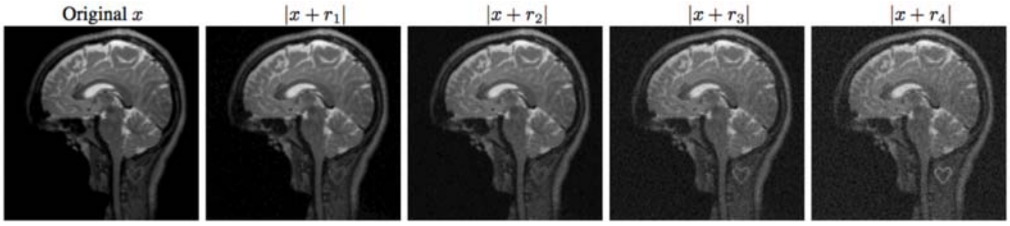

State-of-the-art

Compressed Sensing

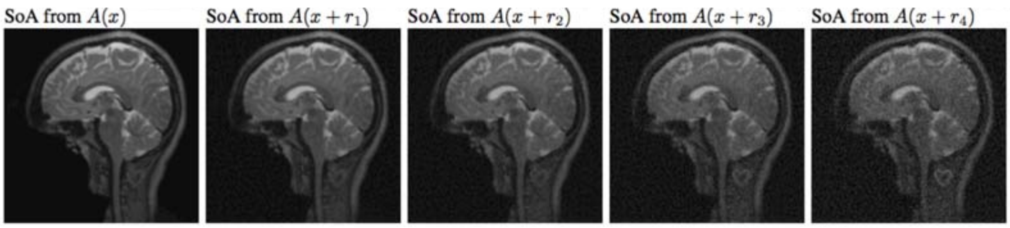

V. Antun, F. Renna, C. Poon, B. Adcock, A.C. Hansen, "On instabilities of deep learning in image reconstruction - **Does AI come at a cost**?", preprint arXiv:1902.05300.

Conclusion: Frontiers in bioimage reconstruction

- Opportunities for learning-based techniques
  - Faster, higher-resolution, lower-dose imaging
- How the newer methods profit from the older ones
- Important open issues

Can we trust the results ?

  - How does one assess **reconstruction quality** ?
    Should be "task oriented"!!!
  - Improving the **stability** of CNNs
  - Theory to guide the design: What is the optimal architecture ?
  - Theory to explain the **regularization** effect of CNNs, and their ability to generalize
- Infrastructure requirements
  - Extensive database of high-quality data (including goldstandard)
  - Development of more **realistic simulators**
    both "ground truth" images + physical forward model
  - **True 3D** CNN toolbox (still missing)

References

Foundations

- M.T. McCann, M. Unser, **Biomedical Image Reconstruction: From the Foundations to Deep Neural Networks**, *Foundations and Trends in Signal Processing*, vol. 13, no. 3, pp. 280-359, December 3, 2019.
- M. Unser and P. Tafti, *An Introduction to Sparse Stochastic Processes*, Cambridge University Press, 2014; preprint, available at `http://www.sparseprocesses.org`.
- M. Unser, J. Fageot, H. Gupta, "Representer Theorems for Sparsity-Promoting ℓ_1 Regularization," *IEEE Trans. Information Theory*, vol. 62, no. 9, pp. 5167-5180, September 2016.
- M. Unser, J. Fageot, J.P. Ward, "Splines Are Universal Solutions of Linear Inverse Problems with Generalized TV Regularization," *SIAM Review*, vol. 59, no. 4, pp. 769-793, December 2017.

Algorithms and imaging applications

- E. Soubies, F. Soulez, M.T. McCann, T.-a. Pham, L. Donati, T. Debarre, D. Sage, M. Unser, "**Pocket Guide to Solve Inverse Problems with GlobalBioIm**," *Inverse Problems*, vol. 35, no. 10, paper no. 104006, pp. 1-20, October 2019.
- E. Bostan, U.S. Kamilov, M. Nilchian, M. Unser, "Sparse Stochastic Processes and Discretization of Linear Inverse Problems," *IEEE Trans. Image Processing*, vol. 22, no. 7, pp. 2699-2710, 2013.
- C. Vonesch, M. Unser, "A Fast Multilevel Algorithm for Wavelet-Regularized Image Restoration," *IEEE Trans. Image Processing*, vol. 18, no. 3, pp. 509-523, 2009.
- M. Guerquin-Kern, M. Häberlin, K.P. Pruessmann, M. Unser, "A Fast Wavelet-Based Reconstruction Method for Magnetic Resonance Imaging," *IEEE Transactions on Medical Imaging*, vol. 30, no. 9, pp. 1649-1660, 2011.
- E. Soubies, M. Unser, "Computational Super-Sectioning for Single-Slice Structured-Illumination Microscopy," *IEEE Trans. Computational Imaging*, vol. 5, no. 2, pp. 24
- M. Nilchian, C. Vonesch, S. Lefkimmiatis, P. Modregger, M. Stampanoni, M. Unser, "Constrained Regularized Reconstruction of X-Ray-DPCI Tomograms with Weighted-Norm," *Optics Express*, vol. 21, no. 26, pp. 32340-32348, 2013.

References (Cont'd)

Deep neural networks

- K.H. Jin, M.T. McCann, E. Froustey, M. Unser, "Deep Convolutional Neural Network for Inverse Problems in Imaging," *IEEE Trans. Image Processing*, vol. 26, no. 9, pp. 4509-4522, 2017.
- M.T. McCann, K.H. Jin, M. Unser, "Convolutional Neural Networks for Inverse Problems in Imaging—A Review," *IEEE Signal Processing Magazine*, vol. 34, no. 6, pp. 85-95, 2017.
- H. Gupta, K.H. Jin, H.Q. Nguyen, M.T. McCann, M. Unser, "CNN-Based Projected Gradient Descent for Consistent CT Image Reconstruction," *IEEE Trans. Medical Imaging*, vol. 37, no. 6, pp. 1440-1453, 2018.
- M. Unser, "A representer theorem for deep neural networks," Journal of Machine Learning Research, vol. 20, no. 110, pp. 1-30, 2019.

Acknowledgments

Many thanks to (former) members of
EPFL's Biomedical Imaging Group

- Dr. Emmanuel Soubies
- Dr. Kyong Jin
- Dr. McCann
- Dr. Pouya Tafti
- Dr. Julien Fageot
- Prof. Emrah Bostan
- Dr. Masih Nilchian
- Prof. Ulugbek Kamilov
- Dr. Cédric Vonesch

and collaborators ...

- Prof. Demetri Psaltis
- Prof. Marco Stampanoni
- Prof. Carlos-Oscar Sorzano
- Dr. Arne Seitz
- ....

- Preprints and demos: http://bigwww.epfl.ch/